	Research and Development Program on Seismic Ground Motion	Ref : SIGMA2-2019-D6-033/1
		Version : 1

On the potential interest of the combination of PSD and RVT in seismic studies for nuclear installations

WORK PACKAGE 6 - G.M. FOR ENGINEERING

AUTHORS		REVIEW		APPROVAL	
Name	Date	Name	Date	Name	Date
Julien Berger *Matthieu Caudron* *Irmela Zentner*	*2019/04/18*	*Yousef Bozorgnia*	10/30/2022	*Emmanuel Viallet* ***Public access*** ⦿ ***SIGMA-2 restricted*** ○	*2023-02-24*

DISSEMINATION: *This document must not be distributed to any person, institution or company other than members of SIGMA-2 steering and scientific committees, except under written formal permission of SIGMA-2 steering committee.*

Document history

DATE	VERSION	COMMENTS
2019/04/18	*0*	*First submitted draft*

Executive summary

This work proposes an application of the Random-Vibration Theory (RVT) and stochastic dynamic approach for the evaluation of floor response spectra in an industrial building. RVT provides tools that enable Engineers to transfer seismic ground motion to in-structure floor response spectra and peak responses. The RVT process determines the Power Spectral Density (PSD) from a given target response spectrum and vice versa. The goal of the work is to compare the RVT process in the generation of floor response spectra against a more standard approach based on time-history analyses.

The RVT methodology builds response analysis in the frequency domain. In consequence, only linear or linear-equivalent structural behavior can be considered. The analyses performed in this study showed that considering steady state response during the strong motion duration is acceptable for stiff structures such as Nuclear Power Plant. In contrast to time history analysis, only one analysis is required to obtain the floor response spectra.

Nevertheless, the RVT methodology presents some limitations:

- non-physical target response spectra could have a limited compatibility with hypothesis of the RVT,
- bad estimation of low and high damping response spectra have to be investigated by further works,
- the method should not be applied if the strong motion duration is very short with respect to the central period of the ground motion.

All recommendations and key steps related to RVT are summed up and aimed towards civil Engineers. This document provides guidance for RVT use in an industrial context.

Contents

Introduction

When performing seismic analysis of industrial installations, seismic demand of nonstructural elements is usually represented through in-structure response spectra, expressed in terms of pseudo-spectral accelerations. Pseudo-spectral accelerations are calculated at the floor levels of the structure where the piece of equipment is located. In nuclear engineering, the design of components requires the determination of the in-structure response spectra. These are generally evaluated by time-history analysis, where the seismic load is defined by a set of response spectrum-compatible time series. There is a huge amount of literature on the generation or selection of spectrum-compatible ground motion (e.g. Baker 2011, Zentner, 2014, 2017, Preumont 1985, Gasparini & Vanmarcke 1976). An alternative way consists in modelling the set of spectrum-compatible time series by a random process.

From a mathematical point of view, a large class of random processes can be more suitably described by a Power Spectral Density (PSD). It is well known that a Gaussian stationary stochastic process is entirely characterized by a PSD. Obviously, the seismic ground motion is a non-stationary process. For this reason, the strong motion duration - where the significant energy of the ground motion is concentrated - and the peak response occurs, should be considered. It is then assumed that the ground motion can be represented by a stationary process during its strong motion duration. However, in earthquake engineering, the seismic ground motion and structural response are generally described by pseudo-acceleration response spectra. The so-called Random Vibration Theory (RVT) allows determining the PSD for a given spectrum and vice versa.

The use of RVT for the computation of floor response spectra has been gaining increasing attention for many years (Igusa & Der Kiureghian 1985, Pozzi & Der Kiureghian 2015, Jiang et al 2015, Heredia-Zavoni 2015, Konakli & Der Kiureghian 2011, Ezeberry & Combescure 2017, Zentner 2018) since it is an interesting alternative to time consuming transient analyses. The tools provided by RVT are also used for the generation of spectrum-compatible ground motion (e.g. Zentner 2014, Preumont 1985, Gasparini & Vanmarcke 1976) and for the introduction of site effects in Probabilistic Seismic Hazard Analysis (PSHA) (Pehlivan et al. 2016, Kottke & Rathje 2013).

In engineering seismology, the RVT is used to transform ground motion PSD into response spectra (Boore & Joyner 1984) and, more recently for host-to-target adjustment (Al Atik et al. 2014).

In earthquake engineering, the RVT is generally used in conjunction with modal correlation coefficients in order to determine peak response quantities from modal maxima (e.g. Heredia-Zavoni 2011; Jiang et al 2015, Pozzi & Der Kiureghian 2015, Igusa et al. 1984, Der Kiureghian 1981). This is called response-spectrum method or spectral analysis.

Igusa and Der Kiureghian (1985) were among the first to combine RVT and modal response spectrum analysis to generate floor response spectra. A limitation of this work comes from the modal response spectrum analysis which involves assumptions (Newmark combination…) to combine seismic responses from each of the single direction input motion in a 3D model. A way to overcome this assumption is to apply RVT for generating a spectrum-compatible PSD of the ground response spectrum, to transfer the PSD inside the structure, and to switch back to in-structure response spectra from the transferred PSDs. Paskalov & Reese (2003) applied such a RVT-stochastic dynamics approach for the computation of in-structure floor spectra of a nuclear power plant. However, their work is based on several simplifying assumptions such as white noise excitation and lacks a clear definition of the equivalent stationary duration to be used for RVT. More recently, Ezeberry & Combescure (2017) applied this approach to compute floor spectra for the ITER Tokamak complex. Cacciola et al. (2004) applied RVT-stochastic dynamics to numerically evaluate the modal correlation coefficients to be used for the response spectrum method. Here, we propose a more complete analysis comparing both the RVT-stochastic dynamics and response spectrum approach to the results of time history analysis. In contrast to former applications of RVT in which the peak observation durations can be non-physical (e.g. Pascalov & Reese, 2003, Boore & Thompson, 2012, Kottke & Rathje, 2013), the duration here is set as the strong motion duration rigorously defined via an energy criterion based on the Arias intensity (Trifunac & Brady, 1974).

The aim of the work is:

- First, to provide some elements on the computation of floor spectra by the RVT-stochastic dynamics approach.
- Second, to present an application to an industrial building and to show the floor response spectra obtained by the two different methods using the same 3D ground motion response spectra:
    - Time history analysis, based on five soil spectrum-compatible time series,
    - RVT-stochastic dynamics approach.

1. Description of the RVT- stochastic dynamic approach

Basic concepts of the RVT are summarized here to understand the following applications of the methodology.

1.1. Computation of floor spectra and peak responses based on RVT

The so-called RVT establishes a link between the standard deviation and the distribution of the maxima of a stationary Gaussian process by means of a peak factor. This topic is also more generally known as the first passage problem and has been studied in the literature since the late sixties by various authors (e.g. Davenport 1964, Crandall et al. 1966, Lin 1967, Udwadia & Trifunac 1974, Vanmarcke 1975). In the framework of earthquake engineering, one takes advantage of the fact that any linear transformation of a Gaussian stochastic process yields a Gaussian stochastic process.

This applies to the response $Z(t) \in \mathbb{R}$ of a linear structure subjected to base excitation by seismic ground motion modelled by the Gaussian stationary process $\ddot{X}(t) \in \mathbb{R}$. The response PSD function $S_Z\ (\omega)$ is obtained by linear filtering of the input $S_{\ddot{X}}(\omega)$ in the frequency domain as:

$$S_Z = h(\omega) S_{\ddot{X}}(\omega) h(\omega)^* \tag{1}$$

The maxima of such a process, observed over a time interval T, are random variables. In particular, the distribution of the maxima of a process obtained as the response of a linear oscillator excited by the floor acceleration time histories $\ddot{z}(t)$ enables one to characterize the distribution of the respective floor response spectrum. As it is common use, we denote a stochastic process by capital letters and particular realizations of it by lower case letters.

One key element for the successful application of RVT is the definition of the duration. We consider time history $\ddot{x}(t)$, $t \in [0, T_d]$, where T_d is the total duration of the non-stationary time history. We need to define the strong motion duration where the time histories are considered as stationary signals and during which the peak values are expected to occur.

The Arias-intensity based on the definition of strong motion duration is adopted here for this purpose. More precisely, the strong motion duration T is the interval between 5% and 95% of Arias intensity of the signal (Trifunac & Brady, 1974):

$$I_a = \frac{\pi}{2g} \int_0^{T_d} \ddot{x}(t)^2 dt \tag{2}$$

It is to be noticed that other definitions of the duration for the RVT are available in PEER report No. 2018/05 (Kottke, et al., 2018) such as one of Bora et al. (2014) that proposes a non-physical duration minimizing the discrepancies between the observed response spectrum and the one calculated from observed Fourier Amplitude Spectra and RVT.

Two major assumptions for the RVT approach to be applicable are linear or, as an extension, equivalent-linear structural behavior, and excitation by a stationary Gaussian process. The strong motion duration of the seismic load defines the equivalent stationary duration for the RVT approach. It is assumed that the steady state regime is reached during this time interval and that the equivalent stationary duration of the response is not significantly different from the input. This assumption is reasonable if the eigenfrequency and modal damping are not too low (Gasparini & Vanmarcke 1976, see also Kottke & Rathje 2013). This is the case for the computation of response spectra for oscillator eigenfrequencies not less than 0.5Hz and 5% damping and when considering the response of rigid structures such as nuclear power plants. The stochastic dynamics approach could be applied to non-stationary ground motion defined by an evolutionary PSD model $S_{\ddot{X}}(\omega, t)$ (e.g. Zentner 2016, Sgobba et al. 2011) as long as the evolution of the PSD is slow with respect to the oscillations (Priestley 1965). The evolutionary structural response then reads:

$$S_Z(\omega, t) = h(\omega) S_{\ddot{X}}(\omega, t) h(\omega)^* \tag{3}$$

but the peak factors would not be applicable anymore.

Moreover, the definition of such a model requires the characterization of the evolution of the frequency content with time (common models consider an evolution of the central frequency) and this data is not available for engineering analysis today. It is also acknowledged that most evolutionary models do not lead to spectrum-compatible ground motion as required here.

The tools provided by RVT allows:

- To determine a PSD in agreement with a given response spectrum by means of the so-called Vanmarcke formula,
- and inversely, to calculate the response spectrum from a given PSD by means of the peak factor.

The computation of floor spectra and peak responses based on the RVT stochastic dynamics approach is illustrated in Figure 1.

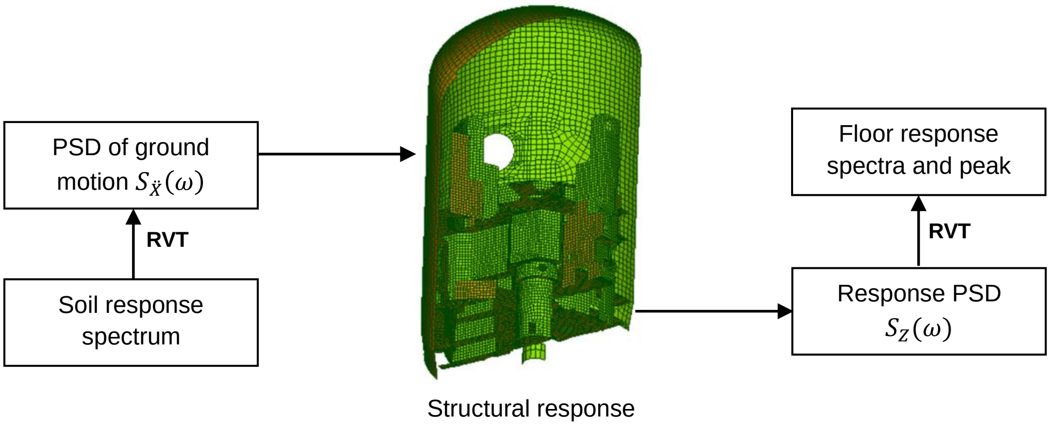

Figure 1: Illustration of the RVT stochastic dynamics approach for the computation of floor response spectra and peak responses

The analysis is performed in the frequency domain using modal synthesis. The stochastic dynamics equations are outlined in what follows for clarity. We consider a linear structure with N degrees of freedom. Given $\boldsymbol{\phi} \epsilon \mathbb{R}^{N\times K}$, the modal matrix containing the K eigenvectors, the vector response is expressed as $\boldsymbol{Z}(\boldsymbol{t}) = \boldsymbol{\phi}\boldsymbol{U}(t)\epsilon\mathbb{R}^N$, where $\boldsymbol{U}(t)\epsilon\mathbb{R}^K$ is the vector containing the modal coordinates. Then, using the diagonal modal transfer function matrix $\widetilde{H}\,(\omega)\epsilon\mathbb{R}^{K\times K}$, the modal response PSD reads

$$\boldsymbol{S_U}(\omega) = \widetilde{\boldsymbol{H}}(\omega)\boldsymbol{S_F}(\omega)\widetilde{\boldsymbol{H}}(\omega)^* \tag{4}$$

where $\boldsymbol{S_F}(\omega)$ is the PSD of the modal seismic load vector $\boldsymbol{F}(t) = -\boldsymbol{\phi}^T\boldsymbol{M}\boldsymbol{I}\ddot{x}(t)\epsilon\mathbb{R}^K$. This vector is determined from the ground acceleration by means of the influence vector $\boldsymbol{I}$, containing the nodal displacements for unitary base movement, and the mass matrix $\boldsymbol{M}$. In consequence, there is no need to apply modal combination rules, the response PSD is expressed in physical coordinates as

$$\boldsymbol{S_Z}(\omega) = \phi\boldsymbol{S_U}(\omega)\phi^T \tag{5}$$

The peak values and response spectra are then deduced directly by means of RVT from the response PSD functions $S_{Z_i}(\omega)\epsilon\,\mathbb{R}, i = 1, \cdots N$ of interest, where $S_{Z_i}(\omega)$ are the i[th] diagonal terms of the response PSD matrix $\boldsymbol{S_Z}(\omega)$. The formula used for the RVT computations are recalled in what follows.

1.2. Evaluation of the response spectrum from a given PSD

More precisely, the RVT allows writing the median pseudo-acceleration response spectrum $\hat{S}_a$ for frequency ω_n and damping ratio ξ_0 as the product of the standard deviation σ_y and the peak factor of a stationary stochastic process $Y(t)$ observed on time interval T:

$$\hat{S}_a = \omega_n^2 \eta_{T,p=0.5} \sigma_y(\omega_n, \xi_0) \quad (6)$$

The peak factor $\eta_{T,p}$ depends on the considered time interval T and the quantile p. When considering median values, $p = 0.5$. According to the recommendations of PEER report No. 2018/05 (Kottke, et al., 2018), the peak factor is estimated by the semi-empirical expression proposed by Gasparini & Vanmarcke (1976), such as:

$$\eta_{T,p}^2 = 2\ln\left(2\eta_p\left[1 - exp\left(-\delta^{1.2}\sqrt{\pi\, ln(2\eta_p)}\right)\right]\right)$$
$$\eta_p = -\frac{v_o^+ T}{\ln(p)} \quad (7)$$

This formula accounts for the fact that the level crossings occur within clumps. It is an improvement over former formulations where the peaks were considered as independent under the assumption of a Poisson process. In the above equations, δ is the bandwidth of the stochastic process $Y(t)$ and T is the strong motion duration. The peak factor depends on the duration. Obviously, when considering a Gaussian process, the longer the period of observation, the higher is the expected maximum. The mean number of zero up-crossings v_0^+ is given by the classical Rice formula (Rice, 1944):

$$v_0^+ = \frac{1}{2\pi}\sqrt{\frac{m_2}{m_0}} \quad (8)$$

and the bandwidth or spreading parameter reads (Vanmarcke, 1972):

$$\delta = \sqrt{1 - \frac{m_1^2}{m_0 m_2}} \quad (9)$$

The mean number of zero up-crossings corresponds to the central frequency, which is the frequency where the energy of the process is concentrated, while the spreading parameter takes values in the range between 0 (no spread) and 1 (wide band process). These parameters depend on the spectral moments m_i of the oscillator response defined as:

$$m_{Y,i}(\omega_n) = \int_{-\infty}^{+\infty} |\omega^i||H_n(\omega)|^2 S_{\ddot{Z}}(\omega)\, d\omega \quad (10)$$

where $\sqrt{m_0(\omega_n)}$ is the standard deviation and the frequency transfer function depends on the eigenfrequency ω_n and damping ratio ξ_0. It reads: $H_n(\omega) = 1/(\omega_n^2 - \omega^2 + 2i\xi_0\omega_n\omega)$.
Since ξ_0 is a fixed value, the reference to this parameter is omitted here and in what follows in order to simplify the mathematical expressions. For the evaluation of equation (7), we can take $v_0^+ = \frac{\omega_n}{2\pi}$ and determine the spreading parameter as (Vanmarcke, 1972):

$$\delta = \sqrt{1 - \frac{1}{1-\xi_0^2}\left[1 - \frac{1}{\pi}\tan^{-1}\left(\frac{2\xi_0\sqrt{1-\xi_0^2}}{1-2\xi_0^2}\right)\right]^2} \quad (11)$$

Relation (11) is obtained with equations (8) and (9) for white noise excitation. It can be further simplified for small critical damping ratio, yielding :

$$\delta \cong \sqrt{\frac{4\xi_0}{\pi}} \tag{12}$$

According to Vanmarcke 1972, the approximate expression is sufficiently accurate as long as $\xi_0 < 0.1$, which is generally the case for response spectra. In consequence, the simplified relation is used in the following applications. Eventually, the standard deviation $\sigma_Y(\omega_n, \xi_0)$ can be easily calculated, for each frequency ω_n, by using equation (10):

$$\sigma_Y(\omega_n, \xi_0) = \sqrt{m_{Y,0}(\omega_n)} \tag{13}$$

1.3. Evaluation of peak responses from the response PSD

Peak responses are evaluated simply by applying the peak factor of equation (7) to the standard deviation of the considered response quantity. In particular: $D_{max} \approx \eta_{T,p=0.5}\sigma_Z$ and $A_{max} \approx \eta_{T,p=0.5}\sigma_{\ddot{Z}}$, where σ_Z and $\sigma_{\ddot{Z}}$ are obtained as the square root of the zeroth moment of the response PSD $S_{\ddot{Z}}(\omega)$ and $S_Z(\omega)$. The peak factor depends on bandwidth and central frequency. These values are determined directly from the moments of the response PSD by using equation (8) and equation (9). The i^{th} moment of the PSD $S_Z(\omega)$ is obtained as $m_{Z,i}(\omega_n) = \int_{-\infty}^{+\infty} |\omega^i| S_Z(\omega) d\omega$.

1.4. Evaluation of the PSD from the given soil response spectrum

In order to express the PSD as a function of the response spectrum by virtue of equation (5), the standard deviation $\sqrt{m_0(\omega_n)}$ has to be expressed as a function of the PSD. For white noise excitation (constant S_X) one obtains, in a first approximation for a filter $H_n(\omega)$ with eigenfrequency ω_n and fixed ξ_0:

$$m_0(\omega_n) = \int_{-\infty}^{+\infty} |H_n(\omega)|^2 S_{\ddot{X}}(\omega) d\omega \cong S_{\ddot{X}}(\omega_n) \int_{-\infty}^{+\infty} |H_n(\omega)|^2 d\omega = \frac{\pi S_{\ddot{X}}(\omega_n)}{2\xi_0\omega_n^3} \tag{14}$$

The above expression is exact for white noise ($S_X(\omega) = const$) and a crude approximation in the general case for frequency-dependent $S_{\ddot{X}}(\omega)$. Formula (14) has been further improved by Vanmarcke who accounts for the actual contribution of $S_X(\omega)$ in the frequency range $[-\omega_n, 0] \times [0, \omega_n]$ where $H_n(\omega) \cong 1/\omega_n^2$:

$$m_0(\omega_n) = \int_{-\infty}^{+\infty} |H_n(\omega)|^2 S_{\ddot{X}}(\omega) d\omega \cong \frac{\pi S_{\ddot{X}}(\omega_n)}{2\xi_0\omega_n^3} + \frac{2}{\omega_n^4}\int_0^{\omega_n} S_{\ddot{X}}(\omega) d\omega - \frac{2}{\omega_n^3} S_{\ddot{X}}(\omega_n) \tag{15}$$

By virtue of equation (6) we can write $\hat{S}_a^2 = \omega_n^4 \eta_{T,p}^2 m_0(\omega_n)$ which, together with relation (12), yields the inverse formula:

$$S_{\ddot{X}}(\omega_n) \approx \frac{1}{\omega_n\left(\frac{\pi}{2\xi_0} - 2\right)} [\frac{\hat{S}_a^2(\omega_n)}{\eta_{T,p}^2} - 2\int_0^{\omega_n} S_{\ddot{X}}(\omega) d\omega] \tag{16}$$

This allows to evaluate the PSD for discrete positive frequencies ω_n. The procedure is initialized by using the white noise approximation of equation (14) instead of (15) and taking the peak factor equal to 1. This approximation is valid for small filter frequencies ω_n. In the following applications, the white noise approximation is used for frequencies lower than 0.1Hz.

2. Simple case studies

The aim is to verify the adequateness of the RVT algorithm described in the previous section thanks to simple case studies. The principle is presented in Figure 2: a spectrum-compatible PSD is evaluated from a target response spectrum through the formulation of §1.4. From this spectrum-compatible PSD, another PSD-compatible response spectrum is calculated in coherence with §1.2. Then, the target response spectrum and the PSD-compatible response spectrum are compared, and the results discussed.

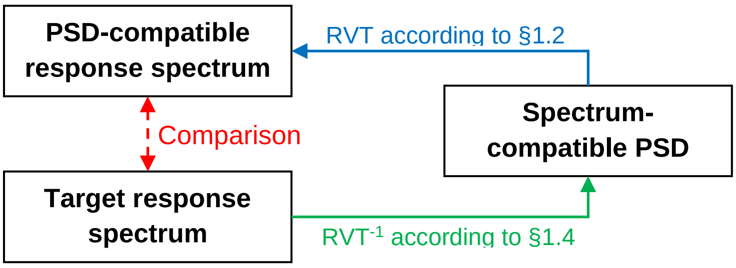

Figure 2: Principle to check the adequateness of the RVT algorithm

The case studies are based on target response spectra available in the literature and defined for different damping ratios. Selected target response spectra come from three formulations for which applicability ranges are reminded in Table 1:

- Response spectra from empirical horizontal Ground-Motion Prediction Equation (GMPE) proposed by Berge-Thierry et al. (2003) and embedded in the French fundamental safety rule RFS2001-01. Scaling parameters are set such as $M_s = 5.42$, $R_{hyp} = 7.0\ km$ for rock sites. According to Pedron (2000), the mean strong motion duration of the seismic scenario is defined as $T_{I_{Arias\,[5-95\%]}} = 4.8\ s$.
- Response spectra from empirical horizontal GMPE proposed by Akkar et al. (2013, 2014). Scaling parameters are chosen as $M_w = 6.5$, $R_{JB} = 7.0\ km$, $V_{S_{30}} = 750\ m/s$ applied to normal faults. This GMPE is particularly interesting since Sandikkaya (2017) provides two definitions of the mean strong motion duration: $T_{I_{Arias\,[5-95\%]}} = 12.1\ s$ and $T_{I_{Arias\,[5-75\%]}} = 5.2\ s$.
- Medium soil EUR response spectra, with Peak Ground Acceleration (PGA) scaled to 0.25g. Strong motion duration is assumed to be $T = 13.0\ s$.

Table 1: Applicability ranges of the GMPEs/spectra

	Berge-Thierry et al. (2003) GMPE	**Akkar et al. (2013, 2014) GMPE**	**EUR spectra**
Frequency	$f \in [0.1, 34\ Hz]$	$f \in [0.25, 100\ Hz]$	$f \in [0.1, 50\ Hz]$
Magnitude	$M_s \in [4.5, 7.3]$	$M_w \in [4.0, 8.0]$	-
Distance	$R_{hyp} \in [7, 100\ km]$	$R_{JB,hyp,Epi} < 200\ km$	-
Soil type	Alluvium sites $V_{S_{30}} \in [300, 800\ m/S]$ Rock sites $V_{S_{30}} > 800\ m/s$	$V_{S_{30}} \in [150, 1200\ m/s]$	Soft, medium and hard
Faults	-	Reverse, normal and strike-slip	-
Damping	$\xi \in [0\%, 30\%]$	$\xi \in [1\%, 50\%]$	$\xi \in [0.5\%, 50\%]$

Moreover, a set of spectrum-compatible time-histories (cf. Figure 3) is generated according to the state of the art by POWERSPEC 2.0 for which the mean 5% response spectrum matches the 5% Berge-Thierry's target spectrum for frequencies higher than 0.25 Hz. The maximal and mean correlation coefficients of the set are respectively 24.7% and 8.5%. Parameters such as strong motion duration, cumulative absolute velocity and Arias intensity are also compatible to Pedron's (2000) predictions. The time-histories should be increased by 3.6% to get a 5% mean response spectrum fully covering the 5% target response spectrum. This coefficient is not considered in this study.

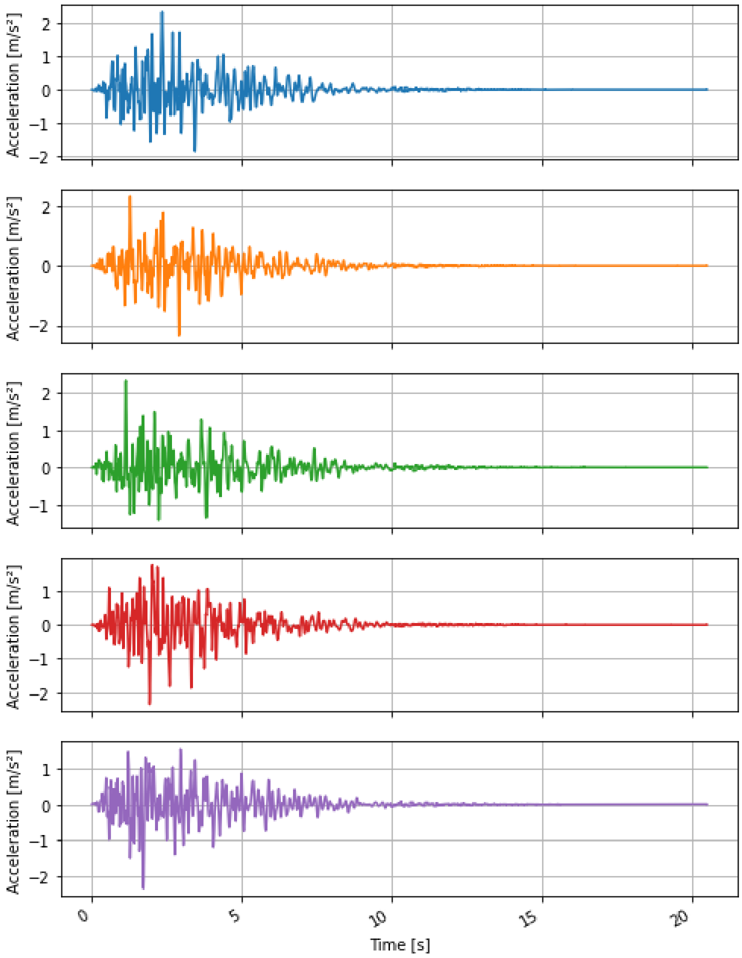

Figure 3: Set of five spectrum-compatible time-histories

2.1. Evaluation of response spectra by RVT at given target damping ratios

Comparing the target spectrum to the spectrum determined from RVT algorithm is a useful and necessary check to assess the adequateness of the spectrum-compatible PSD.
The approach works generally very well when "physical" response spectra, corresponding to possible ground motion, are used. In this case, the input ground motion can be represented by a gaussian stochastic process such that RVT can be applied. Figure 4 illustrates adequate fits when considering either Akkar's (2014) or Berge-Thierry's (2003) target response spectrum with a damping ratio of 1%, 5%, 10% and 30% and a duration parameter sets as the strong motion duration between the Arias Intensity goes from 5% to 95%. Nevertheless, spectrum-compatible PSD evaluated from target response spectra at different damping ratios are not similar for a given GMPE. Such a result is not in agreement with theoretic expectations. The PSD describing the soil ground motion should be unique and should not depend on the damping level of the target response spectrum. The fact that the target

spectrum does not strictly correspond to a gaussian process might be one of the reasons for the observed discrepancies. Moreover, the cutoff frequency of the spectrum-compatible PSD can occur at a lower frequency than that of the target response spectra for higher damping ratios. This is particularly visible on results based on Akkar's GMPE.

For some cases when the target spectrum is a broadened envelope, the frequency content in the middle range (plateau of spectrum) might be incompatible with the PGA (which is the high frequency asymptotic value of the response spectrum). From a mathematical point of view, this means that the standard deviation of the process is not compatible with the assumed peak value and thus the PGA. An example of such a case is shown for the EUR spectra in Figure 4 for damping ratio above 1%.

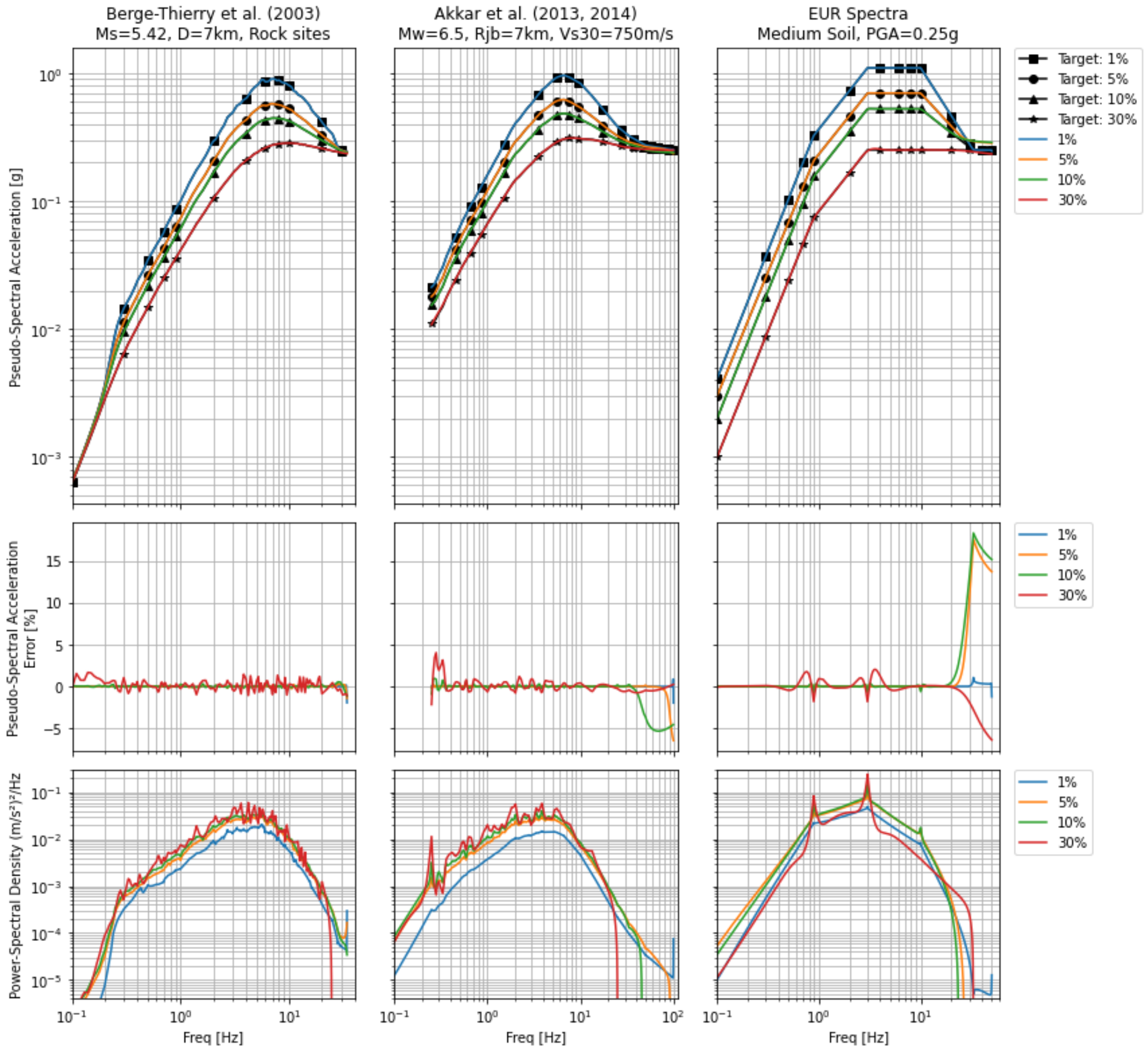

*Figure 4: a) Comparison of target and RVT^{-1}/RVT process' response spectra for four damping ratios b) Pseudo-spectral acceleration error ({[computed/target]-1}*100) for four damping ratios' target response spectra*
c) Spectrum-compatible PSD given by RVT for four damping-ratios' target response spectra

2.2. Evaluation of response spectra at different damping ratios by RVT

The RVT can also be used to obtain response spectra at different damping ratios from the spectrum-compatible PSD. This procedure can be used as an alternative to empirical models such as Rezaeian et al. (2014) or instead of calculating and interpolating floor response spectra at different damping values.

The aim of the case study is to compute pseudo-acceleration spectra at different damping ratios (1%, 5% and 30%) through RVT process from a unique spectrum-compatible PSD. The spectrum-compatible PSD is determined by RVT^{-1} algorithm from a 5% Berge-Thierry's target response spectrum. The results are then compared to pseudo-acceleration spectra given by Berge-Thierry's GMPE and to pseudo-acceleration spectra calculated from a set of five spectrum-compatible time-histories.

Figure 5 presents the results. The calculated 5% response spectra coincide with the Berge-Thierry's target spectrum above 0.25 Hz which validates both RVT^{-1}/RVT and time-histories generation processes. The comparison of response spectra at other damping levels to Berge-Thierry's spectra points out some differences:

- for damping ratio lower than 5%, RVT process gives a response spectrum higher than one provided by Berge-Thierry's GMPE into the overall frequency range (mean error: +29% in the frequency range [0.25, 34 Hz]). Regarding the result of the five time-histories, the mean response spectrum is chaotic but closer to the Berge-Thierry response spectrum (mean error: +5% in the frequency range [0.25, 34 Hz]) with spikes reaching the RVT response spectrum.
- for damping ratio higher than 5%, an opposite behavior is observed: the response spectrum obtained by RVT process are lower than spectrum from Berge-Thierry's GMPE (mean error: -15% in the frequency range [0.25, 34 Hz]. The mean response spectrum of the five time-history oscillates around the Berge-Thierry spectrum with a mean error of +1% in the frequency range [0.25, 34 Hz].

The spectrum-compatible PSD issued from the RVT^{-1} process and calculated from the five time-histories are also compared. The trend of both PSD is similar. However, the amplitude of the PSD given by the RVT^{-1} process is globally higher than one from time-histories. Moreover, PSD calculated from time-histories is chaotic due to the number of time-histories: a smoother PSD trend can be obtained by increasing the number of time-histories.

A sensitivity is also performed on the choice of the damping ratio of target response spectrum allowing to scale the spectrum-compatible PSD. Two spectrum-compatible PSD are then calculated by RVT^{-1} process from target response spectra matching respectively 1% and 30% damping ratios. Response spectra are then calculated by RVT process at 1%, 5% and 30% damping ratio. Figure 6 and Figure 7 show the results obtained respectively from PSD compatible with target response spectra of 1% and 30% damping ratio. Previously observed trends are confirmed with underestimated spectra for damping ratio lower than the one of the target response spectrum used to scale the PSD (and vice versa). Discrepancies can be also noticed on the PGA and the cutoff frequency as observed in the previous paragraph 2.1.

As already mentioned, spectrum-compatible PSD is influenced by the damping ratio of the target response spectrum. The use of extreme damping ratios (e.g. 1 or 30 %) to determine the spectrum-compatible PSD is not recommended when this spectrum-compatible PSD becomes the input data for computing response spectra at other damping ratio (via RVT process). This leads to non-negligible errors in estimations on response spectrum at damping levels other than that of the target response spectrum. However, starting the process with 5% target response spectrum may be a good compromise even if some under-estimations are observed for damping ratio higher than 10%.

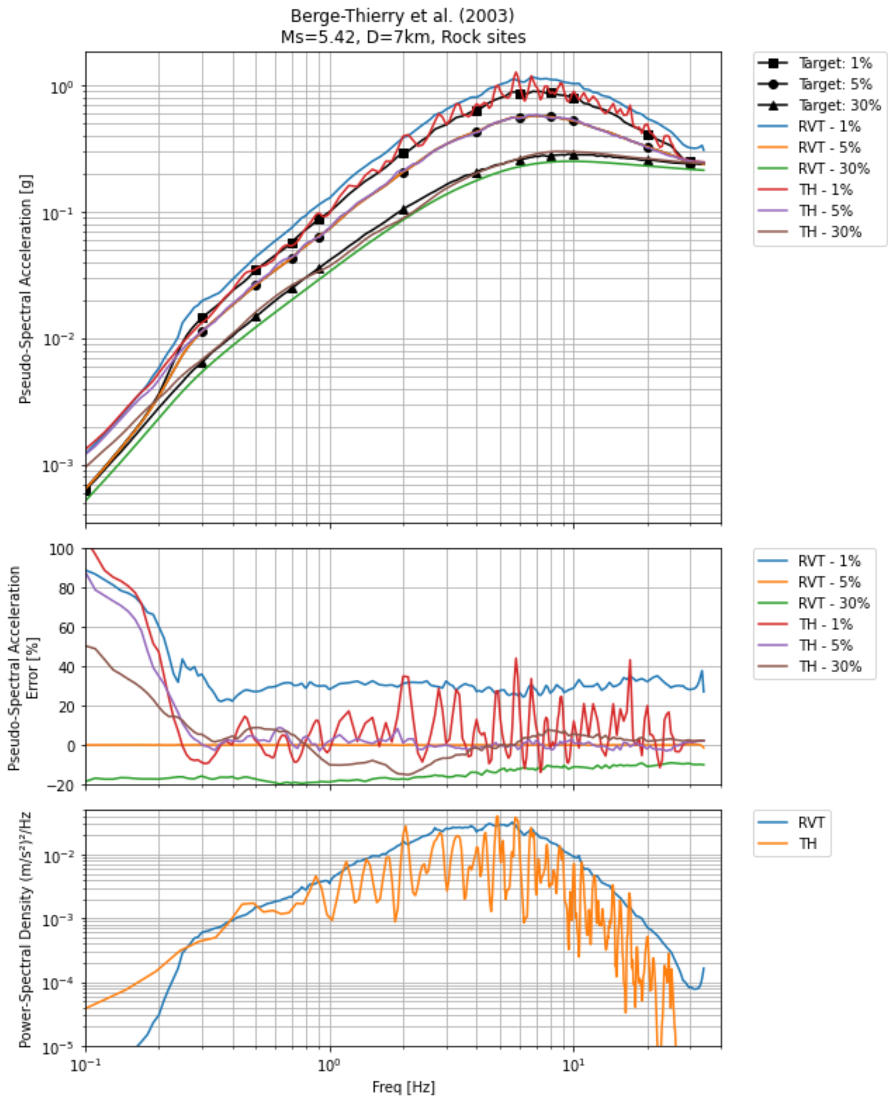

Figure 5: PSD from a 5% target response spectrum
a) Comparison of target, time-history and RVT^{-1}/RVT process' response spectra for three damping ratios' response spectra
*b) Pseudo-spectral acceleration error ({[computed/target]-1}*100) for three damping ratios' target response spectra*
c) Spectrum-compatible PSD given by RVT for three damping-ratios' target response spectra

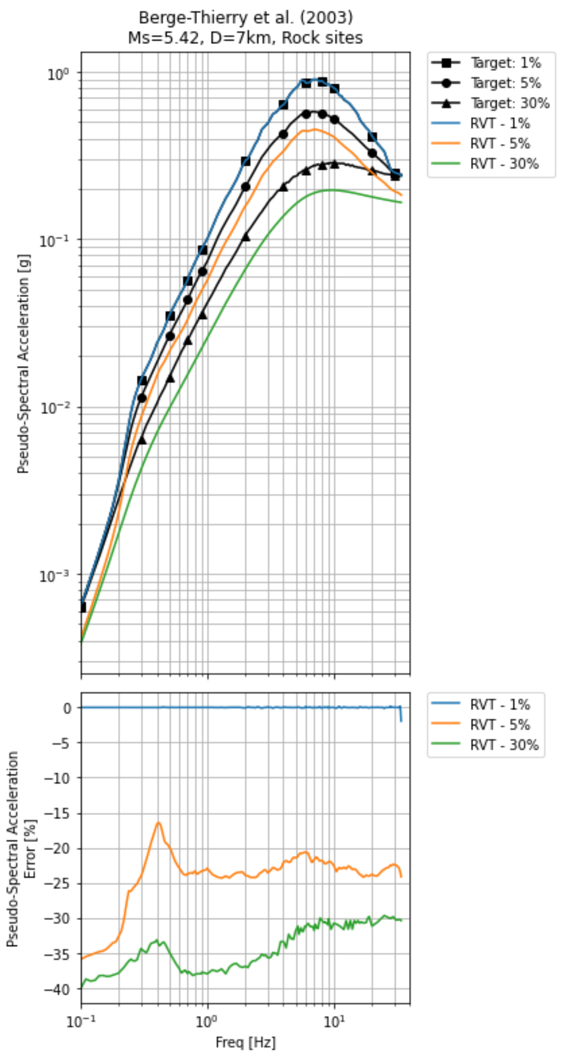

Figure 6: PSD sets to a 1% target response spectrum
a) Comparison of target and RVT-1/RVT process' response spectra for three damping ratios' response spectra
b) Pseudo-spectral acceleration error ({[computed/target]-1}*100) for three damping ratios' target response spectra

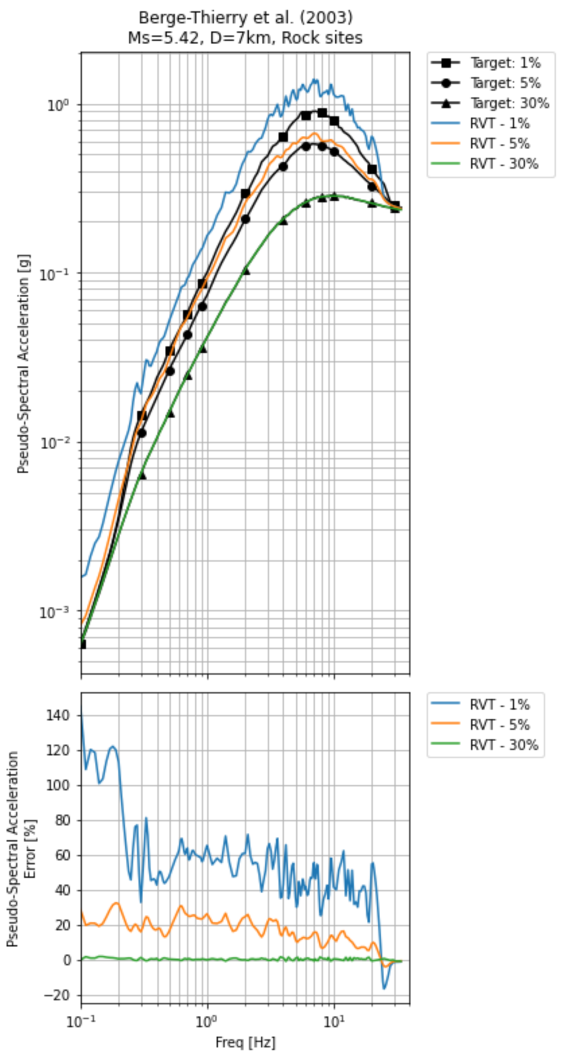

Figure 7: PSD sets to a 30% target response spectrum
a) Comparison of target and RVT-1/RVT process' response spectra for three damping ratios' response spectra
b) Pseudo-spectral acceleration error ({[computed/target]-1}*100) for three damping ratios' target response spectra

2.3. Sensitivity to the duration parameter on response spectra

A key for the RVT process is the duration parameter which is defined here as the strong motion duration evaluated into the interval between the Arias Intensity goes from 5% to 95% [*eq.(1)*]. The aim is to perform sensitivity analyses of this parameter.

Sandikkaya et al. (2017) provides predictive models for Akkar's GMPE according to two definitions of the strong motion duration: time interval between the Arias Intensity goes from 5% to 95% and from 5% and 75%. Regarding the scaling parameters of the Akkar's GMPE presented in §2 ($M_w = 6.5$, $R_{JB} = 7.0\ km$, $V_{s_{30}} = 750\ m/s$), the duration decreases from 12.1s for the former definition, to 5.2s for the latter. Spectrum-compatible PSD are calculated according to a 5% Akkar's target response spectrum, for both definitions of the strong motion duration.

Figure 8 compares response spectra obtained at three damping ratios (1%, 5% and 30%) for both durations against response spectra of Akkar's GMPE. Firstly, the same conclusions as for paragraph 2.2 can be drawn when comparing RVT response spectra at a damping ratio of 1% and 30% to ones of Akkar's GMPE. Secondly, the choice of the duration parameter is observable on the response spectra. On one hand, minimizing the duration parameter reduces pseudo-spectral error of extreme damping ratios but on the other hand, the cut-off frequency decreases by 20 Hz.

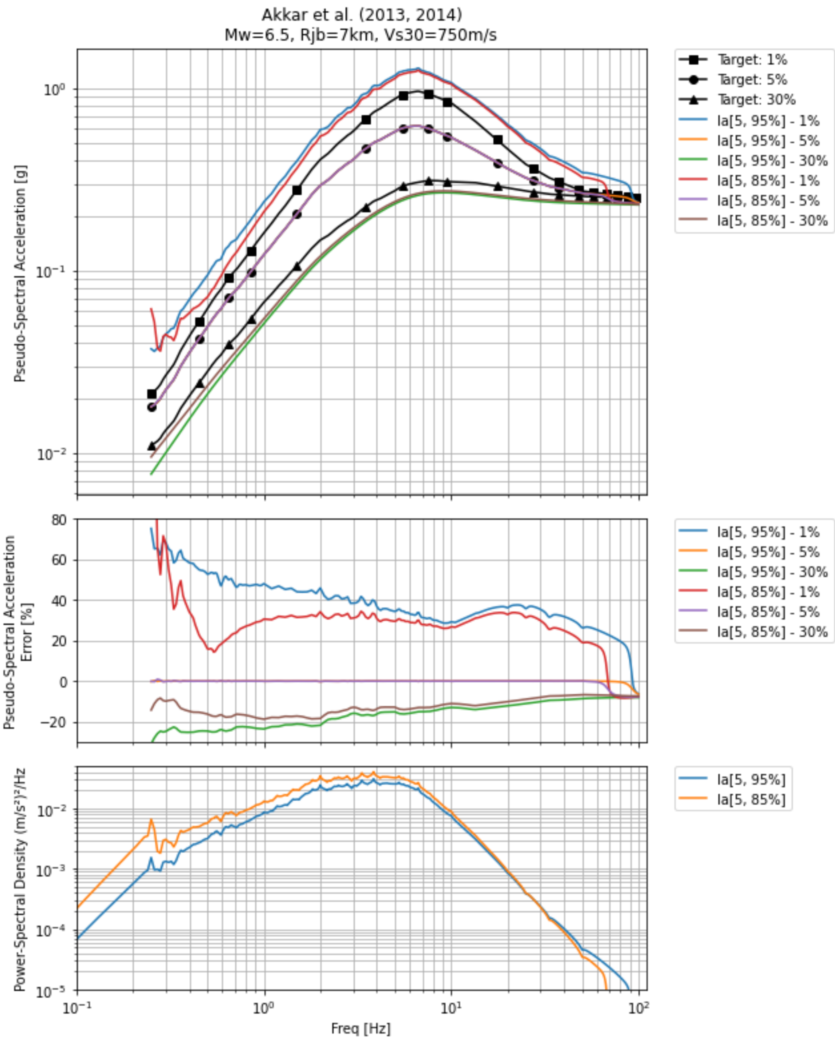

Figure 8: a) Comparison of target and RVT-1/RVT process' response spectra for three damping ratios' response spectra and two duration parameters
*b) Pseudo-spectral acceleration error ({[computed/target]-1}*100) for three damping ratios' target response spectra and two duration parameters*
c) Spectrum-compatible PSD given by RVT for three damping-ratios' target response spectra and two duration parameters

2.4. Sensitivity to central frequency of the input motion

The difference between the central period of the input motion and the peak observation duration can lead RVT process to provide bad estimation in results. The aim is to give an order of magnitude of the minimal peak observation duration needed to get accurate results. This duration will be of course dependent on the central period of the input motion.

For that, the Berge-Thierry's ground-motion excitations expressed in terms of time-series and PSD are transferred to single degree-of-freedom systems calibrated at eigen-frequencies whose periods represent 5, 9, 12 and 50 times the 5-95% Arias intensity' Strong Motion Duration (SMB). Damping ratios of 1%, 5%, 10% and 30% are considered for each of the four single degree-of-freedom systems. To avoid any bias in the RVT^{-1}/RVT processes, PSD and peak response are scaled with the same damping ratio as for the damping ratio of the studied single degree-of-freedom system (cf. §2.1).

Figure 9 compares the response spectra after transferring ground-motion PSD and the five time-series through the single degree-of-freedom systems. The results of the single degree-of-freedom systems with a damping ratio of 1% shows chaotic pseudo-spectral errors that tend to be reduced when the eigen frequency of the system increases. Regarding results at other damping ratios, a strong motion duration 10 times higher than the central period of the input excitation seems to give reduced pseudo-spectral errors between RVT and time series methods. These comparisons suggest an RVT process not suitable for very lightly damped structures or for very short strong-motion durations (with respect to the central period of the input motion). However, the order of magnitude should be refined by comparing RVT results with results coming from more than five partially uncorrelated time-history analyses.

Some differences between time-history and RVT processes are also noticed on the transferred response spectra with a damping ratio of 5% dispite a perfect match between the spectrum-compatible time-series and PSD presented in paragraph 2.2. We can deduct an evolution of the peak observation duration of a responding oscillator upstream and downstream of the transfer matrix of a single degree-of-freedom system.

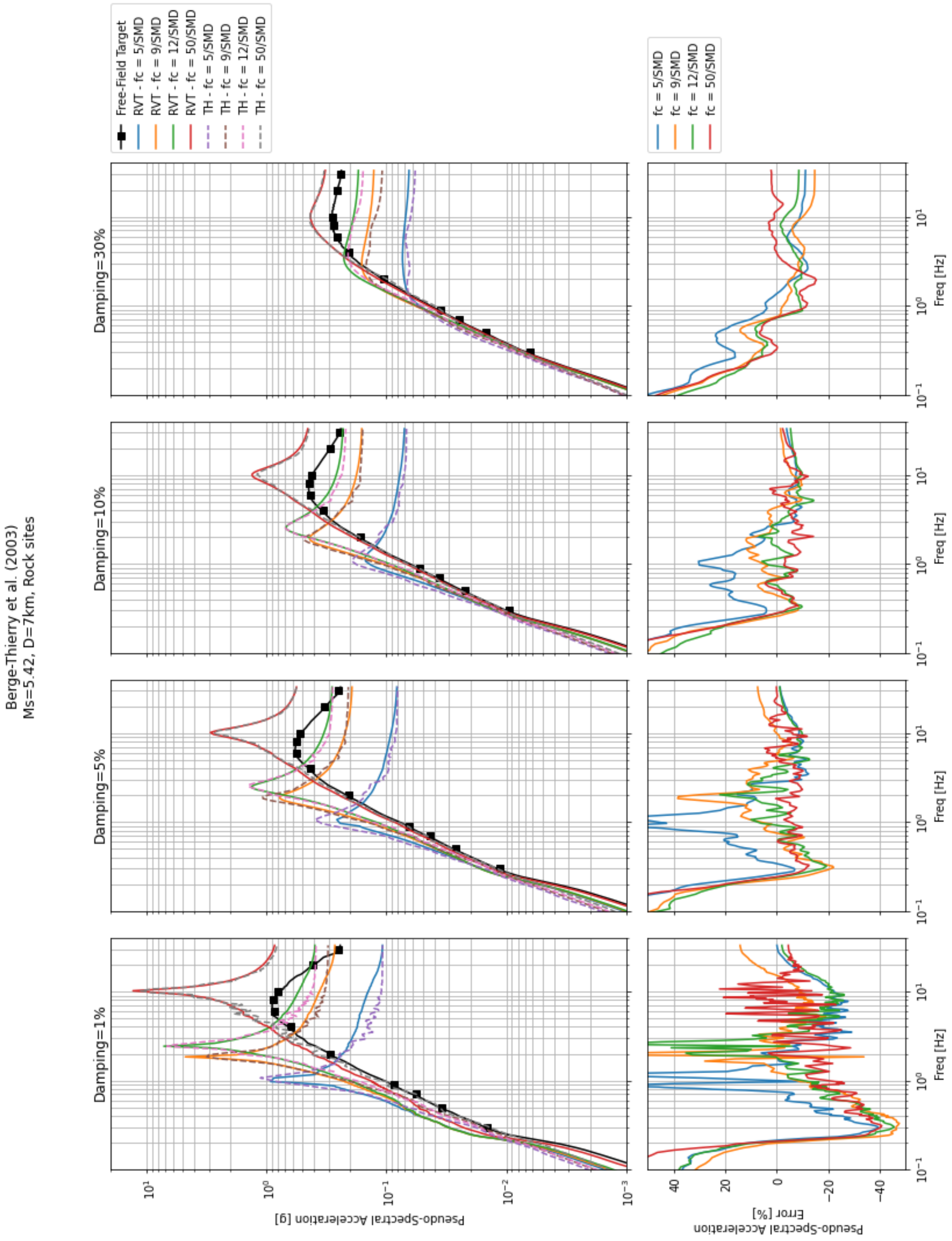

Figure 9: a) Comparison of time-history and RVT process' response spectra after the transfer in a single degree-of-freedom system set for four eigen frequencies and four damping ratios – Ground-motion target response spectrum in black
*b) Pseudo-spectral acceleration error ({[RVT/TH]-1}*100) for three damping ratios' target response spectra*

2.5. Sensitivity to direction interactions

Depending on the dynamic behavior of the studied structure, 3-D seismic motion could interact directionally when computing in-structure response spectra. The directional interactions are embedded in the RVT process through the transfer function $h(\omega)$ of the structure in eq. (1). The aim of the case study is to evaluate the influence of directional interactions by the RVT process with a spectrum-compatibility PSD on one hand, and by spectrum-compatibility time-history method on the other hand.

X and Y-direction ground motions are defined with an identical 5% target response spectrum provided by Berge-Thierry GMPE scaled to parameters of paragraph 2. Directional combinations are expressed by the matrix $h(\omega)$ given in appendix 1 and provided by a cantilever frame of equal lengths L, clamped at its base with a rotational stiffness k_θ and supporting a lumped mass M at its free end (cf. Figure 10). The parameters are calibrated to have a first natural frequency at 10 Hz. The modal damping is set to 5%.

The spectrum-compatible PSD and the uncorrelated artificial time histories are identical to the ones presented in paragraph 2.2. Five sets of three time-histories are created by circular permutations of the five artificial time histories. Each of the five sets are transferred to the cantilever frame's free end thanks to the transfer matrix $h(\omega)$.

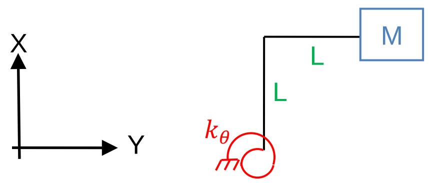

Figure 10: Sketch of the cantilever frame

Figure 11 shows the 5% response spectra obtained at the lumped mass by both RVT and time-history methods. Response spectra of time-history method correspond to the mean response spectra of the five sets for both X and Y directions. Regarding RVT process, an identical response spectrum is computed for X and Y directions due to the symmetry of the cantilever frame's transfer function $h(\omega)$.

A good conformity of results is observed:

- At low frequencies: the pseudo-accelerations are in accordance with free-field ones,
- At frequencies close to the first natural frequency (10 Hz) of the cantilever frame, similar pseudo-accelerations are observed between the RVT and the time-history methodologies.

Pseudo-spectral errors between RVT and time-history methodologies are different when considering X or Y direction. This is due to the variation of the mean correlation between the sets of time-histories obtained by circular permutations. Moreover, the mean correlations of sets are low but not nil. On the other hand, RVT process takes the assumption of "perfect" uncorrelated input motions through the evaluation of a median response spectrum (cf. §1.3 – $p = 0.5$). For information, response spectrum of the cantilever frame obtained from "perfect" correlated input motions $(\rho = -1)$[1] are plotted in Figure 11.

[1] When considering a correlation $\rho = 1$, response spectrum of the cantilever frame is identical to that of the free field input motion.

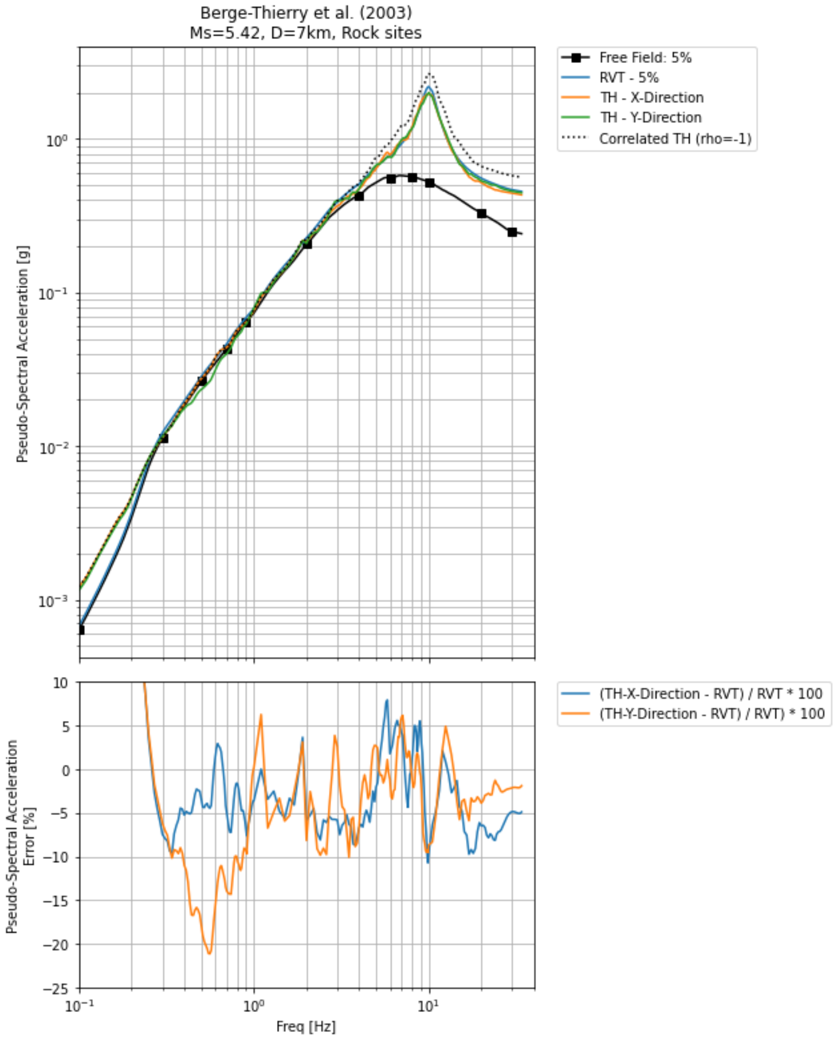

*Figure 11: a) Comparison of time-history and RVT process' floor response spectra Ground-motion response spectrum in black line – Correlated response spectrum in black dotted line b) Pseudo-spectral acceleration error ({[TH/RVT]-1}*100) for four damping ratios' target response spectra*

2.6. Lessons learnt from simple case studies

The differences observed in the simple case studies reinforce the concept of a distinct duration of the input-motion excitation and the duration of a responding oscillator both for the stochastic method of ground-motion simulation as suggested by Boore and Thompson (2012, 2015) and for the floor response spectra evaluation from in-structure transferred PSD.

The duration of a given responding oscillator may not be necessarily the same for converting the ground-motion response spectra to a ground-motion PSD and for converting the transferred ground-motion PSD to floor response spectra since the transfer matrix of the structure may have an impact. Non-physical duration minimizing the discrepancies between the observed ground-motion response spectrum and the one calculated from observed Fourier Amplitude Spectra and RVT as suggested by Bora et al. (2014) might not be applicable after transferring the ground-motion excitation to multi-degree of freedom systems. For this reason, only physical duration defined as the duration between 5 and 95% of the Arias intensity is considered in the section of the industrial case study pending further research work. Moreover, the results coming from oscillator/structure whose eigenfrequencies are less than 0.5Hz and/or with damping ratio less than 5% damping should be carefully interpreted.

3. Industrial case study: computation of floor response spectra

The industrial case study concerns the computation of the floor response spectra of a reactor building induced by a ground motion target response spectrum. The objective is to compare response spectra calculated from the RVT with that calculated from time-history methodology. Computational steps are synthetized in Figure 12.

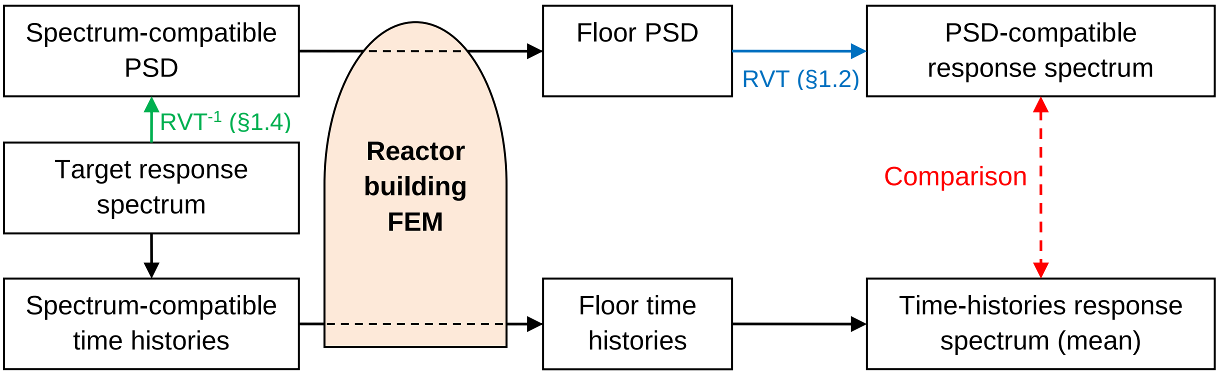

Figure 12: Steps to compare floor response spectra

The linear structural model presented in Figure 13 is a simplified representation of the reactor building. It is composed of a superficial rigid foundation meshed by shell elements, and stick models representing the internal structures (stick n°1) and the containment building (stick n°2). Both sticks are overlapping. The model also includes a frequential Soil-Structural Interaction. Seismic input loads are located at the top (free field) of a firstly-degraded soil column. Structural damping of the building is set at 5%.

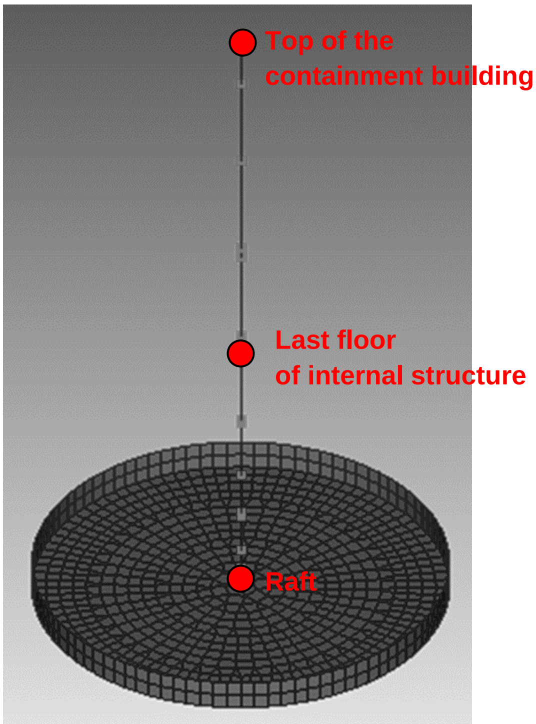

Figure 13: Reactor building finite element model

The code_aster opensource FEM software is used to carry out the analyses:

- for performing the RVT/RVT^{-1} process,
- for transferring spectrum-compatible ground motion PSD and time histories to the reactor building.

The code MISS3D is coupled to code_aster software for the modeling of the frequencial Soil-Structural Interaction. The calculated impedances of the soil are presented in appendix 2.

The analysis is carried out by considering frequencies in the range 0 to 50Hz (~1.5 times the cut-off frequency of the target free field spectrum). Table 2 provides a brief description of the modal basis of the clamped reactor building. Thirty-three eigenmodes are computed in the frequency range [0, 50 Hz].

Table 2: Description of the modal basis
Clamped Reactor Building

Mode n°	Frequency [Hz]	Modal Mass [%]			Description
		X-Direction	Y-Direction	Z-Direction	
1	4.07	27.72%	0.00%	0.00%	1st bending mode of the Containment Building
2	4.07	0.00%	27.70%	0.00%	1st bending mode of the Containment Building
3	5.05	26.87%	0.00%	0.00%	1st bending mode of the Internal Structure
4	5.07	0.00%	26.99%	0.00%	1st bending mode of the Internal Structure
5	12.11	0.00%	0.00%	32.79%	1st vertical mode of the Containment Building
6	12.87	0.00%	5.83%	0.00%	2nd bending mode of the Internal Structure
7	12.88	0.00%	0.00%	30.63%	1st vertical mode of the Internal Structure
8	12.92	6.15%	0.00%	0.00%	2nd bending mode of the Internal Structure
9	13.27	0.00%	5.83%	0.00%	2nd bending mode of the Containment Building
10	13.27	5.71%	0.00%	0.00%	2nd bending mode of the Containment Building
11	20.76	0.00%	0.32%	0.00%	/
12	22.65	0.23%	0.00%	0.00%	/
13	23.42	0.87%	0.00%	0.00%	/
14	23.42	0.00%	0.85%	0.00%	/
15	26.14	0.26%	0.00%	0.00%	/
16	27.65	0.00%	0.00%	2.49%	/
17	27.70	0.00%	1.06%	0.00%	/
18	27.70	0.98%	0.00%	0.00%	/
19	27.91	0.00%	0.29%	0.00%	/
20	35.41	0.64%	0.00%	0.00%	/
21	36.49	0.00%	0.82%	0.00%	/
22	36.69	0.78%	0.00%	0.00%	/
23	36.70	0.00%	0.52%	0.00%	/
24	41.49	0.09%	0.00%	0.00%	/
25	41.59	0.00%	0.07%	0.00%	/
26	43.85	0.00%	0.00%	0.00%	/
27	44.06	0.00%	0.00%	0.00%	/
28	45.21	0.00%	0.00%	0.61%	/
29	45.34	0.33%	0.00%	0.00%	/
30	45.34	0.00%	0.33%	0.00%	/
31	46.20	0.26%	0.00%	0.00%	/
32	46.20	0.00%	0.25%	0.00%	/
33	46.82	0.00%	0.00%	2.45%	/
Sum		**70.87%**	**70.87%**	**68.97%**	100% corresponds to the total mass of the model including the clamped rigid raft

3D-excitations were considered where the vertical loading represents 2/3 of the horizontal one. The seismic scenario is given by Berge-Thierry GMPE scaled to $Ms = 5.42$ and $R_{hyp} = 7km$ for a rock site. The spectrum-compatible PSD and the uncorrelated artificial time histories are identical to ones presented in paragraph 2. Five sets of three time-histories are created by circular permutations of the five artificial time histories

Both RVT and time-history computations are performed by modal synthesis. Floor response spectra are evaluated at the raft (Figure 14), the last floor of the internal structure (Figure 15) and the top of the containment building (Figure 16). Response spectra computed for time-history methodology are the mean of the response spectra of five sets.

Regarding the 5% damping ratio which is identical to the damping ratio of the target response spectrum, the floor response spectra obtained by RVT stochastic dynamics approach at the raft, the last floor of the internal structure and the top of the containment building are close only at high frequencies to the ones determined by transient analysis. Differences are more visible at low frequencies. This is due to the damping ratios of the SSI modes that are higher than the structural damping of 5%: spectrum-compatible PSD is determined from a 5% target spectrum whereas main SSI modes of the building have damping mode higher than 5% (cf. impedances of the soil in appendix 2). Potential issues in changing damping ratio in the RVT process were already discussed in paragraph 2.2.

Whatever the floor, the RVT stochastic dynamics approach provides spectra at damping levels lower than 5% which are globally envelope of time history ones. On the contrary, higher damping response spectra, especially at a damping of 30%, show that RVT method is not necessarily conservative if transient results are taken as reference. RVT and transient results give good concordance for 10% damping response spectra. Some discrepancies are noticed at the raft and the top of the containment building respectively on the cutoff frequency and on the horizontal Zero Period Acceleration (ZPA). Again, this can be explained from the differences between the 5% spectrum-compatible PSD and damping ratio of main SSI modes higher than 5%. (cf. § 2.2)

It is to be noticed that the transfer functions of the reactor building presented in appendix 2 indicate negligible coupling between different directions.

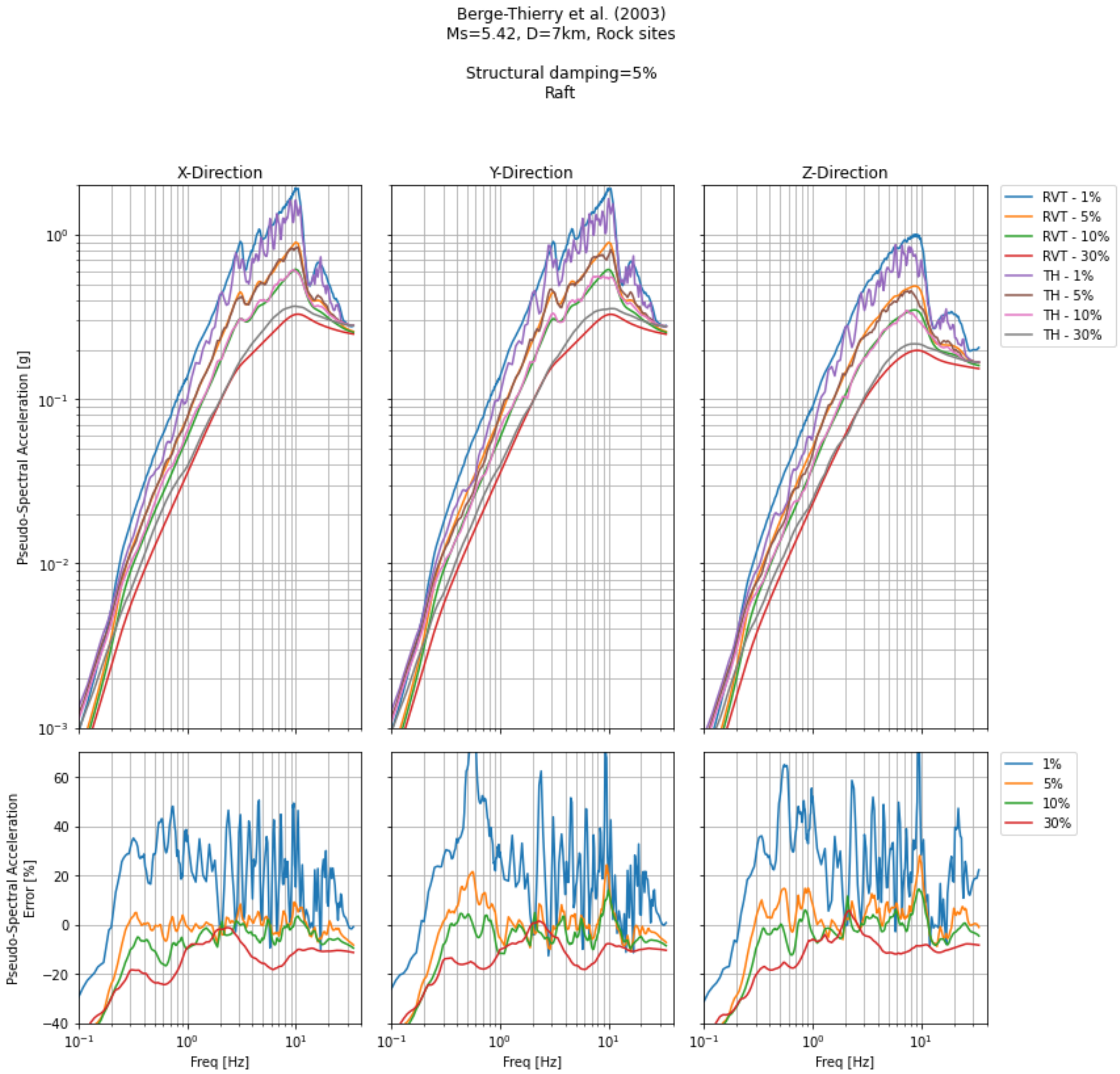

Figure 14: Floor response spectra at the raft
a) Comparison of time-history and RVT process' floor response spectra
*b) Pseudo-spectral acceleration error ({[RVT/TH]-1}*100) for four damping ratios' target response spectra*

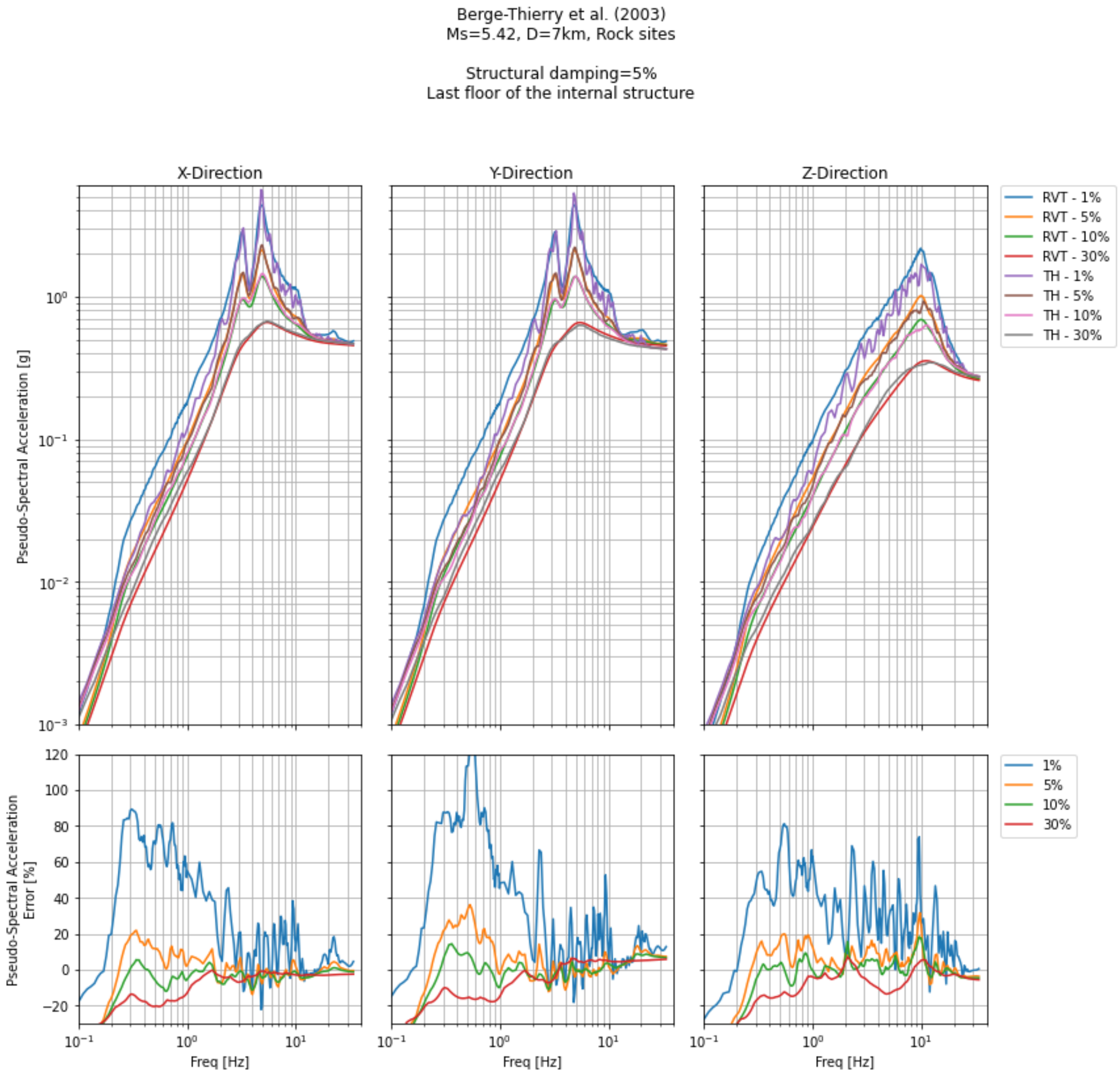

Figure 15: Floor response spectra at the last floor of the internal structure
a) Comparison of time-history and RVT process' floor response spectra
*b) Pseudo-spectral acceleration error ({[RVT/TH]-1}*100) for four damping ratios' target response spectra*

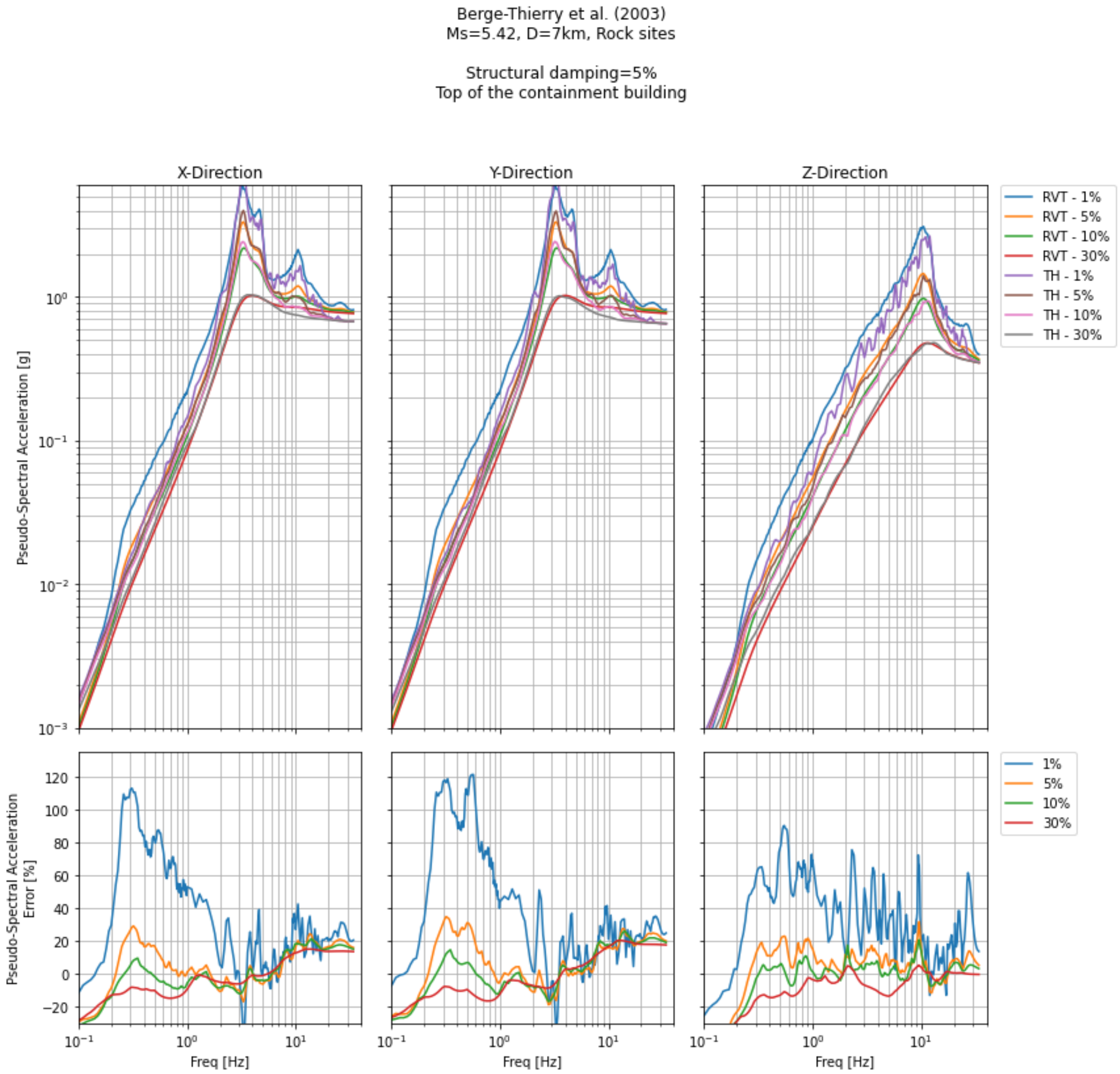

Figure 16: Floor response spectra at the top of the containment building
a) Comparison of time-history and RVT process' floor response spectra
*b) Pseudo-spectral acceleration error ({[RVT/TH]-1}*100) for four damping ratios' target response spectra*

4. Recommendations to civil Engineers for the use of RVT in industrial studies

As shown previously, hypotheses taken for RVT can greatly change its domain of validity. This section proposes guidance for structural Engineers to use the RVT approach in industrial studies, as best as possible.

1) Firstly, spectrum-compatible PSD shall be determined with a 5% target spectrum. This damping ratio guarantees the computation of an envelope or a coherent floor response spectra compared to the usual time history method until damping levels up to ~8-10%. RVT-based evaluation of response spectra with a damping level lower than 1% could be highly conservative. For the evaluation of higher damping floor response spectra, Engineers should probably define an additional spectrum-compatible PSD from a 20 or 30 % target spectrum. However, above-mentioned limitations must be investigated and corrected by further works.

2) Secondly, the definition of the duration is a key parameter. The strong motion duration should be evaluated by using the interval between the Arias Intensity goes from 5% to 95%. The method should not be applied if the strong motion duration is very short (<~10 times) with respect to the central period of the ground motion. In general, the strong motion duration is the same for the input and for the output. However, this is not true anymore for lightly damped structures, and special care should be taken from engineers. Further works must be carried out to allow users to have different strong motion duration for input and output in such cases.

3) In any case, input response spectra determined from RVT algorithm shall be compared to the target response spectrum in order to assess the adequateness of the spectrum-compatible PSD. No issue is generally encountered for “physical” soil response spectra. However, Engineers should pay attention to broadened envelope target spectrum for which the frequency content in the middle range (level of plateau of spectrum) might be incompatible with the Peak Ground Acceleration (PGA, high frequency asymptotic value of the response spectrum).

4) Keep in mind that the RVT approach is based on frequency domain response analysis. Consequently, Engineers shall only apply RVT methodology on linear structural behavior. The method can be extended to nonlinear structures by assuming linear equivalent structural model such as proposed e.g. in Jha et al. (2017) or under development by Nguyen et al. (2016). In the first reference, nonlinear behavior of structures and associated damping are estimated from nonlinear static pushover analysis. Another approach to this issue makes use of stochastic linearization such as proposed in Giaralis & Spanos (2010).

5) At the end of the process, Engineers have at their disposal, for verifying the design of supported equipment, seismic demand expressed in terms of:

   - in-structure response spectra for which classical methodologies can be used (e.g. US NRC 2006),
   - in-structure PSD that can be directly used for seismic analyses of the supported equipment by the stochastic dynamics approach. Another way is to generate time histories from the in-structure PSD. For this purpose, Engineer should pay attention to potential correlation between directions during the generation of such time histories. These points are not treated in the present report.

5. Conclusion

The stochastic dynamics approach is based on the calculation of a spectrum-compatible PSD. The PSD fully defines the underlying stationary stochastic process by providing its energy as a function of frequency. When considering seismic ground motion, an equivalent stationary duration has to be defined. This can be achieved by considering the strong motion duration as defined by the time interval between the Arias Intensity goes from 5% to 95%. The mathematical framework of the so-called RVT provides tools that enable the Engineer to transfer seismic ground motion to in-structure floor response spectra and peak responses. In contrast to time history analysis, only one analysis is required to obtain the floor spectra.

In-structure floor response spectra are used as seismic demand for the design and verification of equipment located in the supporting structure. RVT approach can be used to evaluate the latter quantities at different damping values. The analyses showed that considering steady state response during the strong motion duration is acceptable for stiff structures such as Nuclear Power Plant.

Nevertheless, some limitations were highlighted such as non-physical target spectra that were not in agreement with RVT hypotheses. Bad estimation of high damping response spectra must be investigated and corrected by further works. The extension of the methodology to very lightly damped structures requires also complementary analyses. Finally, the method should not be applied if the strong motion duration is very short with respect to the central period of the ground motion.

The RVT approach is based on frequency domain response analysis. Consequently, only linear structural behavior can be considered. However, the method can be extended to nonlinear structures by assuming linear equivalent structural model or the use of stochastic linearization.

The last part of this document provides a set of guidance for the civil Engineers on the best use of the RVT in an industrial framework. It is to be noted that some important points are still under investigation and should be clarified in a near future.

References

Akkar S., Sandıkkaya M.A, · Bommer J.J (2014), Empirical ground-motion models for point-and extended-source crustal earthquake scenarios in Europe and the Middle East, *Bulletin of Earthquake Engineering.* doi 10.1007/s10518-013-9461-4.

Akkar S., Sandıkkaya M.A, · Ay B. Ö. (2014), Compatible ground-motion prediction equations for damping scaling factors and vertical-to-horizontal spectral amplitude ratios for the broader Europe region, *Bulletin of Earthquake Engineering* **12**:517–547. doi 10.1007/s10518-013-9537-1.

Al Atik, L., Kottke, A., Abrahamson, N., and Hollenback, J. (2014). Kappa (k) scaling of ground motion prediction equations using an inverse random vibration theory approach. *Bulletin of the Seismological Society of America*, 104(1), 336–346.

ASN/GUIDE/2/01 (2006) Guide de l'ASN – Prise en compte du risque sismique à la conception des ouvrages de GC d'installations nucléaires de base à l'exception des stockages à long terme des déchets radioactifs.

Baker, J.W., (2011) *Conditional mean spectrum: tool for ground motion selection*, *J of Structural Engineering.* 137(3) 322 – 331.

Berge-Thierry C., Cotton F., Scoti O., Griot-Pommera, D.A., Fukushima Y. (2003), New Empirical Response Spectral Attenuation Laws For Moderate European, *Journal of Earthquake Engineering*, 193-222.

Bora SS., Scherbaum F., Kuehn N., Stafford P. (2014) *Fourier spectral and duration models for the generation of response spectra adjustable to different source, propagation, and site conditions*, Bull. Earthquake Eng., 12(1): 467-493.

Boore D.M., Joyner W. B. (1984), A note on the use of random vibration theory to predict peak amplitudes of transient signals. *Bulletin of the Seismological Society of America* 74(5), 2035-2039.

Boore, D.M., Thompson E.M. (2012), Empirical improvements for estimating earthquake response spectra with random vibration theory. *Bulletin of the Seismological Society of America* 102(2), 761-772.19.

Boore D.M., Thompson E.M. (2015). Revisions to some parameters used in stochastic-method simulations of ground motion. *Bulletin of the Seismological Society of America*, 105(2a): 1029-1041.Boore D.M., Thompson E.M. (2015).

Cacciola P., Colajanni P. and Muscolino G. (2004) Combination of modal responses consistent with seismic input representation, *Journal of Structural Engineering, ASCE* 130, 47-55.

Clough R.W., Penzien J. (1975) *Dynamics of Structures*. McGraw-Hill.

Crandall SH, Chandiramani KL, Cook RG. (1966) Some first passage problems in random vibrations, *Journal of Applied Mechanics (ASME),* 33 532-538.

Code_aster multi-purpose opensource FEM software, http://www.code-aster.org.

Davenport A.G. (1964), Note on the distribution of the largest value of a random function with application to gust loading. *Proc. Inst. Civ. Eng*., 28, 187-196.

Der Kiureghian, A. (1981) A response spectrum method for random vibration analysis of MDF systems. *Earthquake Eng. Struct. Dyn*. 9, 419– 435.

EUR, "European Utility Requirements for LWR Nuclear Power Plants", Vol. 2, Generic nuclear island requirements, Chapter 4, Design Basis (Part 2), Revision C, April 2001

Ezeberry J, Combescure D. (2017), A direct method for determining floor response spectra at the ITER Tokamak Complex. *Nuclear Engineering and Design*, in press.

Gasparini D.A., Vanmarcke E.H. (1976) Simulated earthquake motions compatible with prescribed response spectra. SIMQKE User's manual and documentation. MIT Report R76-4.

Gerardin, M., Rixen, D., (1994) Mechanical vibrations: Theory and application to structural dynamics. Wiley, Chichester, UK.

Giaralis A. and Spanos P.D., (2010) Effective linear damping and stiffness coefficients of nonlinear systems for design spectrum based analysis. *Soil Dynamics and Earthquake Engineering* 30, 798-810.

Heredia-Zavoni, E., Santa-Cruz, S., and Silva-González, F. L. (2015) Modal response analysis of multi-support structures using a random vibration approach. *Earthquake Engineering and Structural Dynamics* 44, 2241–2260. doi: http://dx.doi.org/10.1002/eqe.2581.

Heredia-Zavoni E. *(*2011), The complete SRSS modal combination rule*. Earthquake Engineering and Structural Dynamics* 40*,* 1181–1196*.*

Igusa T*,* Der Kiureghian A*,* Sackman JL*. (*1984*)* Modal decomposition method for stationary response of non-classically damped systems*. Earthquake Engineering and Structural Dynamics* 12*,* 121–136*.*

Igusa T., Der Kiureghian A. (1985) *Generation of floor response spectra including oscillator structure interaction*, journal of Earthquake Engineering and Structural Dynamics, Vol 13, no. 5, pp.661-676, https://doi.org/10.1002/eqe.4290130508.

Jha N., Roshan A.D., Bishnoi L.R. (2017), Floor response spectra for beyond design basis seismic demand, *Nuclear Engineering and Design*, in press, https://doi.org/10.1016/j.nucengdes.2017.01.006.

Jiang W., Li B., Xie W-C, Pandey M.D. (2015), Generate floor response spectra: Part 1. Direct spectra-to-spectra method, *Nuclear Engineering and Design* 293, 525-546, https://doi.org/10.1016/j.nucengdes.2015.05.034.

Konakli, K. and Kiureghian, A. D. (2011), Extended MSRS rule for seismic analysis of bridges subjected to differential support motions. *Earthquake Engng. Struct. Dyn*., 40, 1315–1335.

Kottke A., et al. (2018) *Selection of Random Vibration Procedures for the NGA-East Project*. PEER Report 2018/05, University of California.

Kottke A., Rathje M. (2013) Comparison of Time Series and Random-Vibration Theory Site-Response Methods. *Bulletin of the Seismological Society of America* 103 (3) 2111-2127; DOI: 10.1785/0120120254.

Lin Y.K. (1967) Probabilistic Theory of of Structural Dynamics. Mc Graw Hill, New York. Menun, C., Reyes, J. C., and Chopra, A. K. (2015) Errors caused by peak factor assumptions in response-spectrum-based analyses. *Earthquake Engng Struct. Dyn*., 44, 1729–1746. doi: 10.1002/eqe.2552.

Nguyen A., Labbé P., Semblat JF., Hervé G. (2016), Systematic analysis of the concept of equivalent linear behavior in seismic engineering by minimization in the frequency domain. TINCE conference, Paris.

Paskalov A., Reese S. (2003), Deterministic and probabilistic floor response spectra, *Soil Dynamics and Earthquake Engineering* 23(7), 605-618.

Pedron C. (2000), Caractérisation de signaux sismiques reels et lois de correlation “Magnitude-Distance” d’indicateurs potentiels de nocivité, CEA report ref. SEMT/EMSI/RT/00-028/A.

Pehlivan, Rathje, Gilbert (2016) Factors influencing soil surface seismic hazard curves. *Soil Dynamics and Earthquake Engineering* 83,180–190.

Pozzi, M., Der Kiureghian, A. (2015), Response spectrum analysis for floor acceleration. *Earthquake Engng Struct. Dyn*., 44, 2111–2127.

Preumont A. (1985), The generation of non-separable artificial earthquake accelerograms for the design of nuclear power plants. Nuclear Engineering and Design 88, 59-67.

Priestley M.B. (1965), Evolutionary spectra and nonstationary processes. J.Royal Statistical Society 27(2), 204–237.

Rezaeian S., Bozorgnia Y., Idriss I. M., Abrahamson N., Campbell K., Silva W. (2014), Damping Scaling Factors for Elastic Response Spectra for Shallow Crustal Earthquakes in Active Tectonic Regions: “Average” Horizontal Component. *Earthquake Spectra* 30(2), 939-963.

RFS2001-01 (2001), Basic safety rule - Fundamental safety rule n°2001-01 concerning basic nuclear installations.

Rice, S. O. (1944), Mathematical analysis of random noise. Bell System Tech. J. 23, 282–332. Rice SO.

Sandikkaya A., Akkar S. (2017), Cumulative absolute velocity, Arias intensity and significant duration predictive models from a pan-European strong-motion dataset, *Bulletin of Earthquake Engineering* **15**,1881–1898. doi 10.1007/s10518-016-0066-6

Sgobba S., Stafford P.J., Marano G.C., Guaragnella C. (2011), An evolutionary stochastic ground-motion model defined by a seismological scenario and local site conditions, *Soil Dynamics and Earthquake Engineering* 31(11), 1465-1479.

Trifunac M.D., Brady A. G. (1974), A study on the duration of strong earthquake ground motion. *Bulletin of the Seismological Society of America 65(3), 581-626* 21.

Udwadia F. E., Trifunac M. D. (1974), Characterization of response spectra through the statistics of oscillator response. *Bulletin of the Seismological Society of America 64(1)*, 205-219.

US NRC (2006) Regulatory Guide 1.92, Revision 2. Washington, D.C.: U.S. Nuclear Regulatory Commission.

Vanmarcke E.H. (1972) Properties of spectral moments with applications to random vibration. *J Engrg. Mech. Div. ASCE* **98,** 425-446.

Vanmarcke E.H. (1975) On the distribution of the first passage time for normal stationary random processes. *ASME J of Applied Mechanics*.

Zentner, I. (2014) A procedure for simulating synthetic accelerograms compatible with correlated and conditional probabilistic response spectra. *Soil Dynamics and Earthquake Engineering* 63, 226-233.

Zentner I. (2018), Use of RVT for Computation of In-Structure Response Spectra and Peak Responses and Comparison to Time History and Response Spectrum Analysis, *Earthquake Spectra,* Vol. 34, No. 4, pp. 1913-1930.

APPENDIX 1: Amplitude of the cantilever frame transfer functions

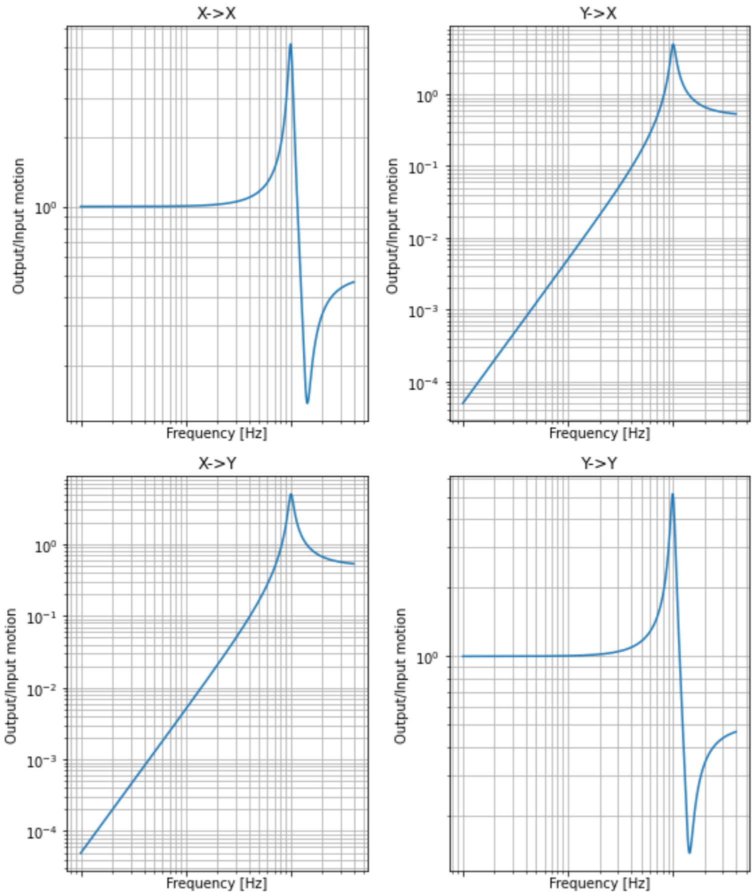

Figure 17: Amplitude of the transfer functions between the free field and the mass of the cantilever frame

APPENDIX 2: Impedances of the soil and transfer functions of the reactor building FEM

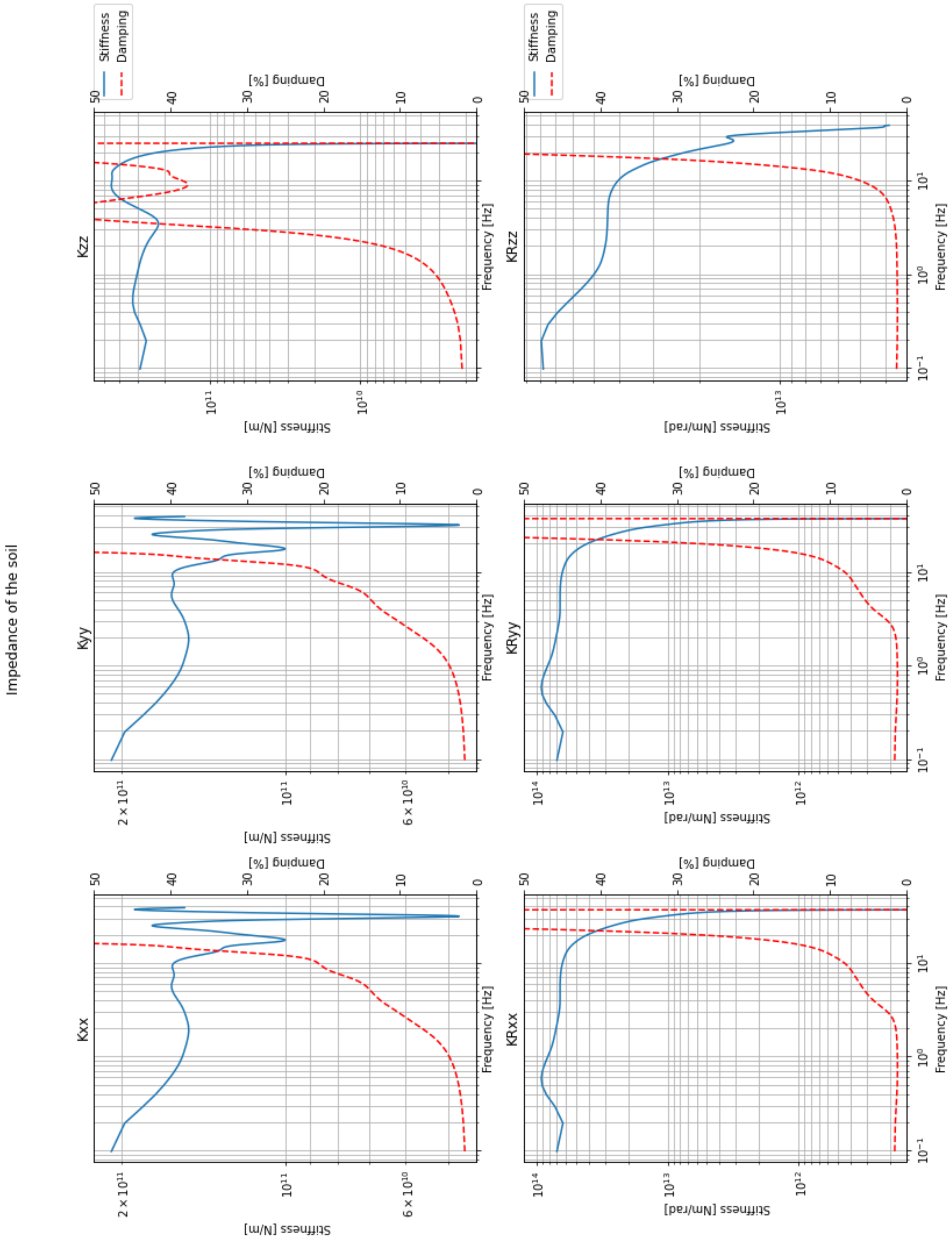

Figure 18: Impedance of the soil

Raft

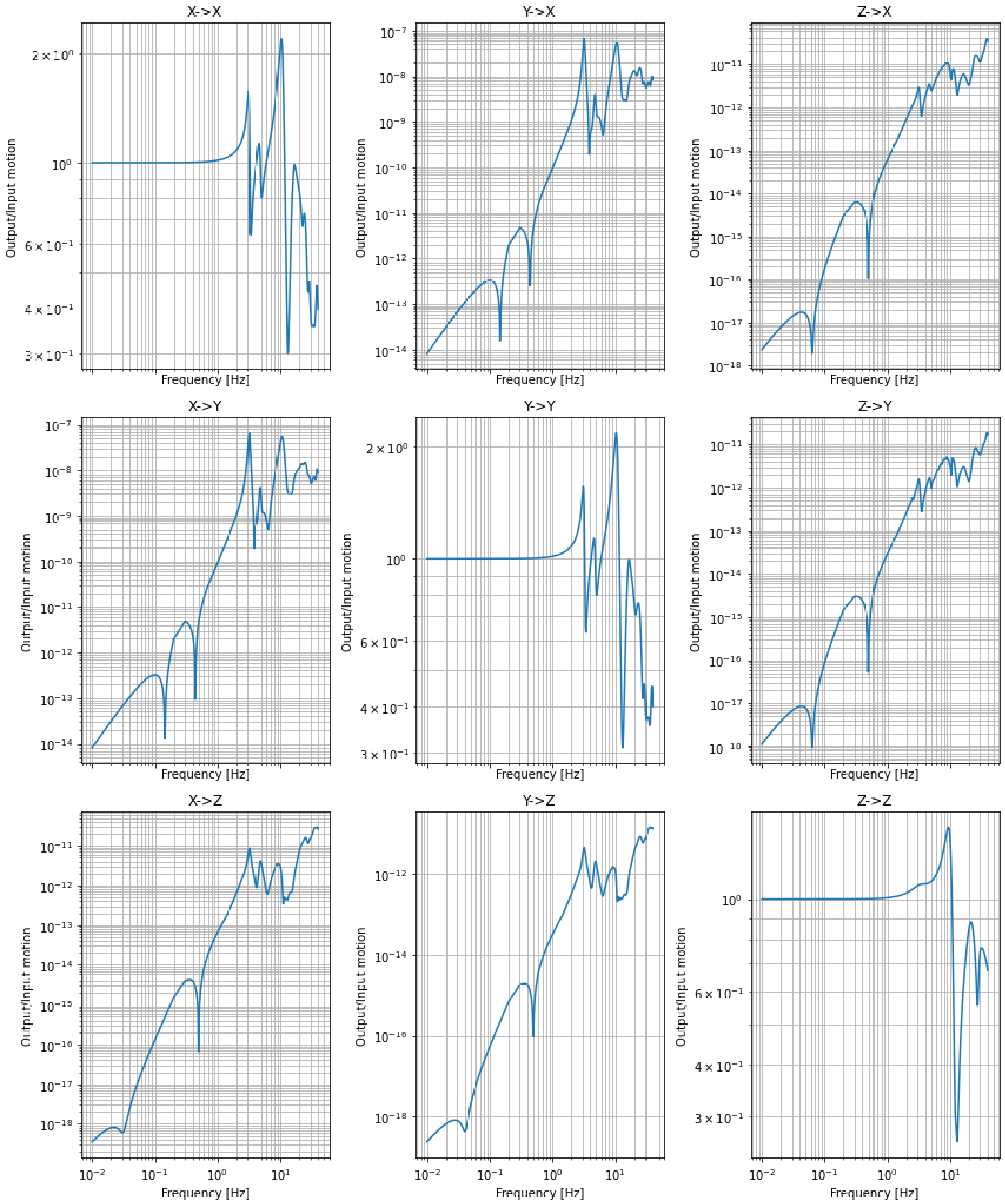

Figure 19: Amplitude of the transfer functions between the free field and the raft

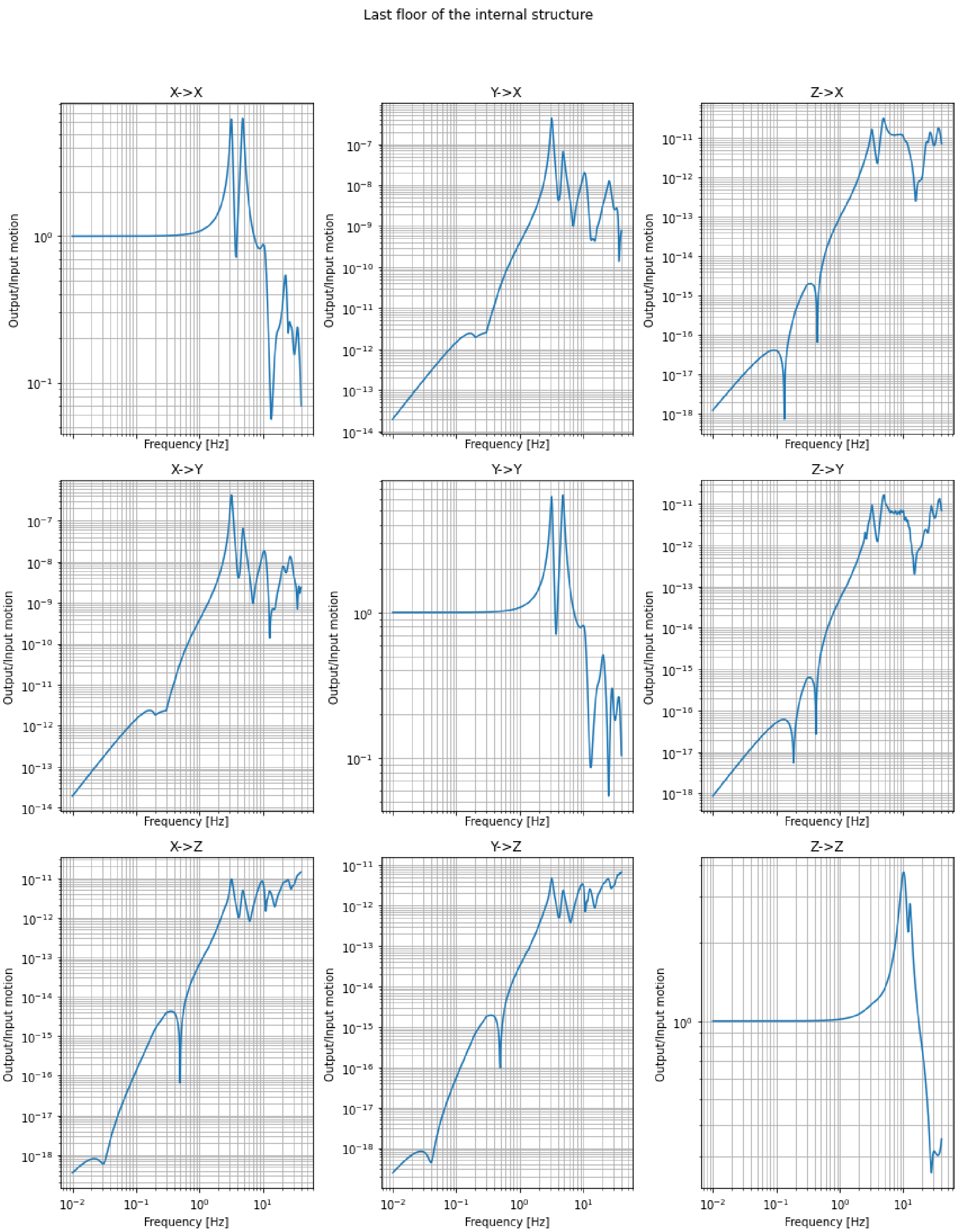

Figure 20: Amplitude of the transfer functions between the free field and the last floor of the internal structure

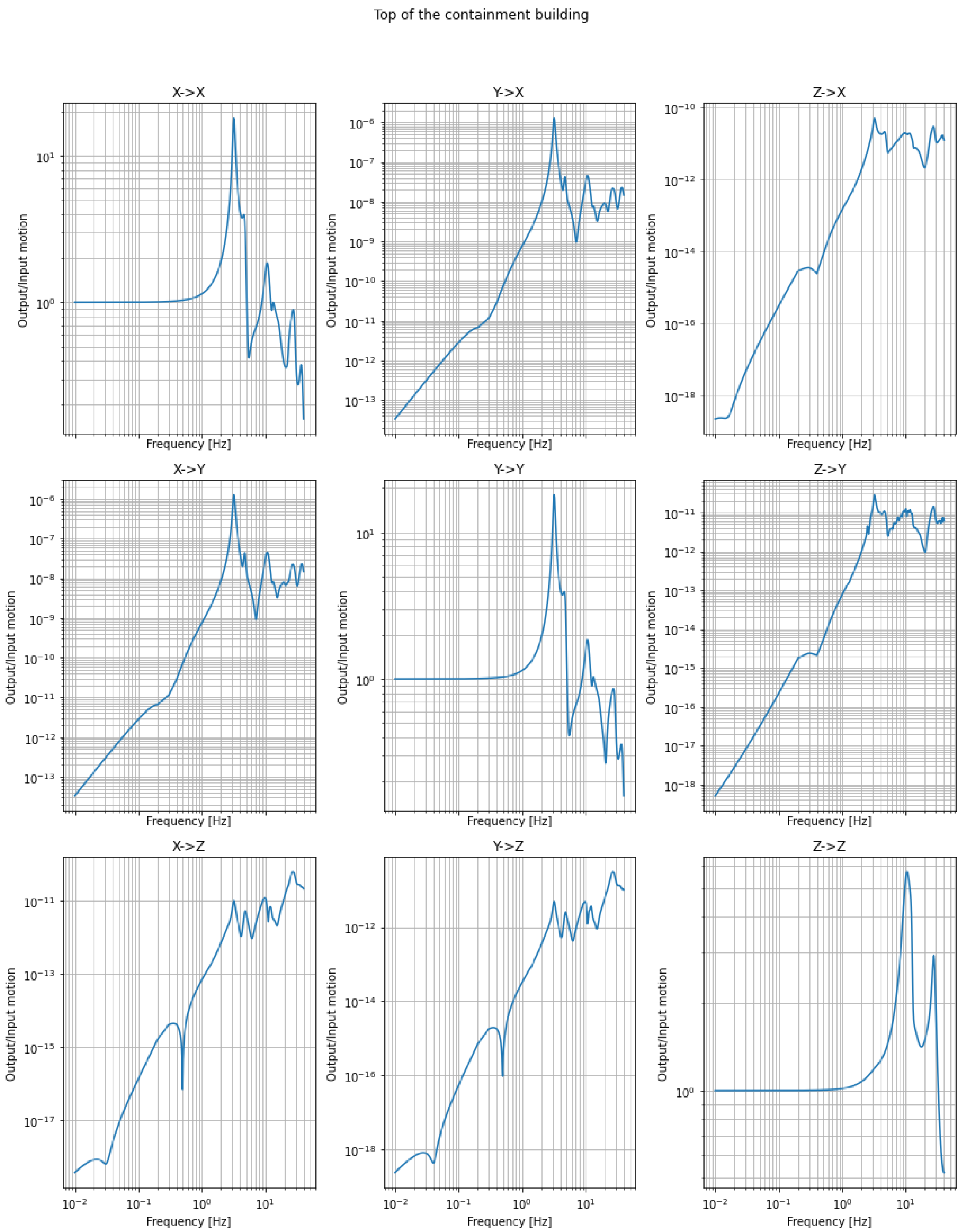

Figure 21: Amplitude of the transfer functions between the free field and the top of the containment building